Hindawi
Advances in Condensed Matter Physics
Volume 2019, Article ID 5639487, 16 pages
https://doi.org/10.1155/2019/5639487

Research Article

Josephson Current through a Quantum Dot Connected with Superconducting Leads

Satoshi Kawaguchi

Department of Complex and Intelligent Systems, School of Systems Information Science, Future University Hakodate, Hakodate 041-8655, Japan

Correspondence should be addressed to Satoshi Kawaguchi; satoshi@fun.ac.jp

Received 26 June 2019; Revised 20 August 2019; Accepted 23 August 2019; Published 18 November 2019

Academic Editor: Oleg Derzhko

In this study, we consider the Josephson current in a system composed of a superconductor/quantum dot/superconductor junction. In the model, the Coulomb interaction in the quantum dot is taken into consideration, and the Lacroix approximation is applied to study the electron correlation. We derive Green's function of the quantum dot by applying the Lacroix truncation. Although the Andreev bound state does not occur in our formulations, the π-junction occurs for a restricted parameter range. On comparing the Kondo temperature with that estimated by another method, it is found that our Lacroix approximation does not capture well the Kondo physics in the superconductor/quantum dot/superconductor junction.

1. Introduction

In the last few decades, the Josephson current in a system composed of a superconductor/quantum dot/superconductor (S/QD/S) junction has been extensively studied [1–4]. When identical superconducting leads are separated by a thin layer of insulator, the Josephson current can flow because of the coherent tunneling of Cooper pairs across the insulator in the absence of a potential difference. When the tunneling amplitude across the barrier is small and the spin is conserved, the current depends on the superconductor phase difference θ between the left and right leads. The current is expressed as $J = J_c \sin\theta$, where J_c denotes the critical current, which is proportional to the normal conductance through the barrier [5]. When $\theta = 0$, the Josephson current is zero and the junction is in the ground state. When $\theta = \pi$, the current becomes zero; however, in this case, the junction energy is maximum and it is in an unstable state. Very recently, carbon-nanotube Josephson junction systems have been studied intensively [6–8].

When we consider physics at low temperatures under the Coulomb interaction in the QD, the physical behavior of the system depends on the relative magnitude of the Kondo temperature T_K and the BCS gap Δ [9]. When $T_K \gg \Delta$, the Kondo effect is sufficiently strong to break the Cooper pair at the Fermi level, and the localized spin in the QD is screened; it is expected that a Kondo singlet will be formed. This results in a positive critical current (0-junction). By contrast, when $T_K \ll \Delta$, the Cooper pair is strongly coupled, and the Kondo screening is essentially negligible. In this case, the Cooper pair is subjected to a localized magnetic moment in the QD. When the Coulomb repulsion in the QD is large, the ground state of the QD is a magnetic doublet, and the electrons in a Cooper pair can tunnel one by one via virtual processes. The spin ordering of the Cooper pair is reversed, resulting in a π-junction [3, 10, 11]. The 0-π transition is expected to occur around $T_K \sim \Delta$. The tuning of the π-junction in S/QD/S systems has been studied extensively [3, 12–14].

The current density in the S/QD/S system is composed of two parts: continuous and discrete spectrums. The former (latter) arises from outside (inside) the BCS gap. The current from the continuous current density is calculated by the usual numerical integral. By contrast, the current from the discrete current density is calculated

by applying the complex function theory. The discrete current density arises from the Andreev bound states (ABSs) inside the BCS gap. The ABSs are determined as poles of the QD Green's function, and there is a pair of ABSs $\omega_{\pm}^{0}$ in the absence of Coulomb interaction. In particular, when the energy level of the QD coincides with the Fermi level $\omega_{\mathrm{F}} = 0$, $\omega_{\pm}^{0} = 0$. In this situation, the current jumps discontinuously when the BCS phase difference is $\pm\pi$ [15, 16]. Usually, the current from the discrete current density is much larger than that from the continuous current density.

The Coulomb interaction in the QD is studied by many methods: the numerical renormalization group (NRG) method [17–19], noncrossing approximation [20], quantum Monte Carlo (QMC) method [21–23], and so on. Although the NRG and QMC methods are very precise methods, they are computationally expensive. The simplest method is the Hartree approximation, which corresponds to the zeroth-order approximation. In this method, a two-particle Green's function is truncated by decoupling at the mean-field level. Beyond the Hartree approximation, the Hartree–Fock (HF) approximation is proposed, where up to the first order of the tunneling amplitude is considered. This method was applied to the level-crossing quantum phase transition between the BCS-singlet and the magnetic doublet states [24–27]. The above two approximations can be applied to describe single-particle physics. The higher-order Green's functions are not taken into consideration; therefore, these approximations are not sufficient when we consider Kondo physics [28]. To overcome this defect, the Lacroix approximation has been proposed [29]. In this approximation, a greater higher-order correlation effect is included in the QD Green's function by truncation in the second order. Although the Lacroix approximation suffers from several defects, the mathematical procedures to derive the QD Green's functions are a simple application of the equation of motion. Although there have been many studies on QD systems that employ the Lacroix approximation [28, 30–34], only a few studies have been conducted on the current in S/QD/S systems [33, 35].

From these standpoints, we examine the current in a system composed of an S/QD/S junction with Coulomb interaction by applying the Lacroix approximation. Under second-order truncation and simplification, Green's function of the QD is obtained. Using Green's functions, we calculate the electron occupation number in the QD and the Josephson current. We can observe the π-junction in a restricted parameter range, but our Lacroix approximation does not capture well the competition between the Kondo effect and superconductivity.

2. Model and Formulation

We first introduce the setup of the system and give its Hamiltonian. For the system, Green's functions of the QD and the Josephson current are derived by employing the equation of motion.

2.1. Model and Green's Functions of the QD. We consider a system composed of an S/QD/S junction, where Coulomb interaction exists in the QD. The geometry of the setup is shown in Figure 1. The total Hamiltonian of the system is written as

$$H = H_L + H_R + H_D + H_T, \tag{1}$$

where

$$\begin{aligned} H_\alpha &= \sum_{k,\sigma} \varepsilon_k c_{\alpha,k,\sigma}^{\dagger} c_{\alpha,k,\sigma} + \sum_{k} \left(\Delta_\alpha c_{\alpha,k,\uparrow}^{\dagger} c_{\alpha,-k,\downarrow}^{\dagger} + \mathrm{H.c.} \right), \\ H_D &= \sum_{\sigma} \varepsilon_d d_\sigma^{\dagger} d_\sigma + U n_{d\uparrow} n_{d\downarrow}, \\ H_T &= t \sum_{k,\sigma} \left(c_{L,k,\sigma}^{\dagger} d_\sigma + c_{R,k,\sigma}^{\dagger} d_\sigma + \mathrm{H.c.} \right), \end{aligned} \tag{2}$$

where $\alpha = L, R$ and $\sigma = \uparrow, \downarrow$. H_α represents the superconducting lead α; $c_{\alpha,k,\sigma}$ denotes the annihilation operator of an electron with energy ε_k, wave number k, and spin σ in the lead; the order parameter $\Delta_\alpha = \Delta e^{i\theta_\alpha}$ with the BCS gap Δ and the BCS phase θ_α; H_D represents the QD; d_σ denotes the annihilation operator of an electron with spin σ; and ε_d denotes the QD energy level. The occupation number of an electron in the QD with spin σ is defined by $n_{d\sigma} = d_\sigma^{\dagger} d_\sigma$, and U represents the Coulomb repulsion between electrons with up- and downspins. H_T represents the electron tunneling between the leads and the QD. The coupling strength between electrons in the QD and the leads is defined by $\Gamma_0 = \pi \nu t^2$, where the tunneling amplitude t is real and ν denotes the normal density of states (DOS) at the Fermi level.

To describe the above system, we introduce the 2×2 Nambu representation. We set the spinor field operators as

$$\begin{aligned} \Psi_{\alpha k\sigma} &= \begin{pmatrix} c_{\alpha,k,\sigma} \\ c_{\alpha,-k,\bar{\sigma}}^{\dagger} \end{pmatrix}, \\ \Psi_{\alpha k\sigma}^{\dagger} &= \begin{pmatrix} c_{\alpha,k,\sigma}^{\dagger} & c_{\alpha,-k,\bar{\sigma}} \end{pmatrix}, \\ \Psi_{d\sigma} &= \begin{pmatrix} d_\sigma \\ d_{\bar{\sigma}}^{\dagger} \end{pmatrix}, \\ \Psi_{d\sigma}^{\dagger} &= \begin{pmatrix} d_\sigma^{\dagger} & d_{\bar{\sigma}} \end{pmatrix}, \end{aligned} \tag{3}$$

where $\bar{\sigma} = \downarrow, \uparrow$. Hereinafter, Green's function written with a hat symbol represents a 2×2 matrix. Using the above operators, the retarded (advanced) 2×2 matrix Green's function is defined as $\widehat{G}_{\alpha k\sigma,\beta k'\sigma'}^{r(a)}(t,t') = \mp i\theta(\pm t \mp t') \langle \{ \Psi_{\alpha k\sigma}(t), \Psi_{\beta k'\sigma}^{\dagger}(t') \} \rangle$. The lesser Green's functions are defined as follows:

Figure 1: Schematic diagram of a superconductor/quantum dot/superconductor (S/QD/S) junction. t denotes the tunneling amplitude between the leads and the QD.

$$\widehat{G}^{<}_{\alpha k\sigma,\alpha' k'\sigma'}(t,t') = i\begin{pmatrix} \langle c^{\dagger}_{\alpha',k',\sigma'}(t')c_{\alpha,k,\sigma}(t)\rangle & \langle c_{\alpha',-k',\bar{\sigma}'}(t')c_{\alpha,k,\sigma}(t)\rangle \\ \langle c^{\dagger}_{\alpha',k',\sigma'}(t')c^{\dagger}_{\alpha,-k,\bar{\sigma}}(t)\rangle & \langle c_{\alpha',-k',\bar{\sigma}'}(t')c^{\dagger}_{\alpha,-k,\bar{\sigma}}(t)\rangle \end{pmatrix},$$
$$\widehat{G}^{<}_{d\sigma,\alpha k\sigma}(t,t') = i\begin{pmatrix} \langle c^{\dagger}_{\alpha,k,\sigma}(t')d_{\sigma}(t)\rangle & \langle c_{\alpha,-k,\bar{\sigma}}(t')d_{\sigma}(t)\rangle \\ \langle c^{\dagger}_{\alpha,k,\sigma}(t')d^{\dagger}_{\bar{\sigma}}(t)\rangle & \langle c_{\alpha,-k,\bar{\sigma}}(t')d^{\dagger}_{\bar{\sigma}}(t)\rangle \end{pmatrix}. \tag{4}$$

Employing the equation of motion, we derive all Green's functions. We denote $\widehat{g}^{r}_{d}$ as the retarded Green's function of the QD in the absence of coupling with the leads, and $\widehat{g}^{r}_{\alpha\sigma}$ is denoted as the retarded Green's function of the lead α with spin σ in the absence of coupling with the QD. In the Nambu representation, these functions are written as

$$\left(\widehat{g}^{r}_{d}(\omega)\right)^{-1} = \begin{pmatrix} \omega - \varepsilon_d + i0^{+} & 0 \\ 0 & \omega + \varepsilon_d + i0^{+} \end{pmatrix},$$
$$\widehat{g}^{r}_{\alpha\sigma}(\omega) = -i\pi\nu\rho(\omega)\begin{pmatrix} 1 & \dfrac{\sigma\Delta_{\alpha}}{\omega} \\ \dfrac{\sigma\overline{\Delta}_{\alpha}}{\omega} & 1 \end{pmatrix}, \tag{5}$$

respectively, where a symbol with an overbar represents the complex conjugate of the symbol, and the factor $\rho(\omega)$ is defined as

$$\rho(\omega) = \begin{cases} \dfrac{|\omega|}{\sqrt{\omega^2 - \Delta^2}}, & |\omega| > \Delta, \\ \dfrac{\omega}{i\sqrt{\Delta^2 - \omega^2}}, & |\omega| < \Delta. \end{cases} \tag{6}$$

It is noteworthy that ρ denotes the ordinary BCS DOS for $|\omega| > \Delta$; however, it is imaginary for $|\omega| < \Delta$.

We define Green's functions of the QD with spin σ using the Zubarev notation as

$$\widehat{G}^{r}_{d\sigma}(\omega) = \left\langle\!\left\langle \begin{pmatrix} d_{\sigma} \\ d^{\dagger}_{\bar{\sigma}} \end{pmatrix}; \begin{pmatrix} d^{\dagger}_{\sigma} & d_{\bar{\sigma}} \end{pmatrix} \right\rangle\!\right\rangle$$
$$= \begin{pmatrix} \langle\langle d_{\sigma}; d^{\dagger}_{\sigma}\rangle\rangle & \langle\langle d_{\sigma}; d_{\bar{\sigma}}\rangle\rangle \\ \langle\langle d^{\dagger}_{\bar{\sigma}}; d^{\dagger}_{\sigma}\rangle\rangle & \langle\langle d^{\dagger}_{\bar{\sigma}}; d_{\bar{\sigma}}\rangle\rangle \end{pmatrix}. \tag{7}$$

By using the Dyson equation, we obtain the retarded Green's functions of the QD as

$$\left[\widehat{G}^{r}_{d\sigma}(\omega)\right]^{-1} = \left[\widehat{G}^{(0)r}_{d\sigma}(\omega)\right]^{-1} - \widehat{\Sigma}^{U}_{\sigma}(\omega), \tag{8}$$

where $\widehat{\Sigma}^{U}_{\sigma}(\omega)$ is the self-energy due to the on-site Coulomb interaction. Following references [19, 36], $\widehat{\Sigma}^{U}_{\sigma}(\omega) = U\widehat{F}_{d\sigma}(\omega)[\widehat{G}^{r}_{d\sigma}(\omega)]^{-1}$, where $\widehat{F}_{d\sigma}(\omega)$ is defined as

$$\widehat{F}_{d\sigma}(\omega) = \begin{pmatrix} \langle\langle d_{\sigma}n_{d\bar{\sigma}}; d^{\dagger}_{\sigma}\rangle\rangle & \langle\langle d_{\sigma}n_{d\bar{\sigma}}; d_{\bar{\sigma}}\rangle\rangle \\ -\langle\langle d^{\dagger}_{\bar{\sigma}}n_{d\sigma}; d^{\dagger}_{\sigma}\rangle\rangle & -\langle\langle d^{\dagger}_{\bar{\sigma}}n_{d\sigma}; d_{\bar{\sigma}}\rangle\rangle \end{pmatrix}. \tag{9}$$

In the absence of Coulomb interaction, $\widehat{G}^{(0)r}_{d\sigma}(\omega)$ is given by

$$\left[\widehat{G}^{(0)r}_{d\sigma}(\omega)\right]^{-1} = \left(\widehat{g}^{r}_{d}(\omega)\right)^{-1} - \widehat{\Sigma}^{0}(\omega), \tag{10}$$

where $\widehat{\Sigma}^{0}$ is the noninteracting self-energy, which is calculated by

$$\widehat{\Sigma}^{0}(\omega) = \widehat{T}\left(\widehat{g}^{r}_{\mathrm{L}\sigma}(\omega) + \widehat{g}^{r}_{\mathrm{R}\sigma}(\omega)\right)\widehat{T}, \tag{11}$$

where $\widehat{T} = t\widehat{\sigma}_z$, and $\widehat{\sigma}_z$ denotes the third component of the 2×2 Pauli matrices. Each element of $\widehat{\Sigma}^{0}$ is given in Appendix.

In the presence of Coulomb interaction, it is necessary to calculate $\widehat{\Sigma}^{U}_{\sigma}$ self-consistently. In this study, we derive Green's functions, $\widehat{G}^{r}_{d\sigma}$, under the Lacroix approximation. Although the Lacroix truncation was originally proposed for the Anderson model with normal conducting leads [29], we extend the method to superconducting leads. The detailed derivations are given in Appendix. The final expression of the (11)-component of $\widehat{G}^{r}_{d\sigma}$ is

$$\left[\widehat{G}^{r}_{d\sigma}(\omega)\right]_{11} = \frac{1}{R_{\sigma}(\omega) - U\left(Q_{\sigma}(\omega) + T_{\sigma}(\omega)\right)/P_{\sigma}(\omega)}, \tag{12}$$

where

$$
\begin{aligned}
P_\sigma(\omega) &= \omega - \varepsilon_d - U\left(1 - \langle n_{d\bar{\sigma}}\rangle\right) + 3i\Gamma_0 \\
&\quad + U\left(A_{1\sigma}(\omega) - A_{2\sigma}(\omega)\right), \\
Q_\sigma(\omega) &= \left(\omega - \varepsilon_d - U\langle n_{d\bar{\sigma}}\rangle\right)\left(A_{1\sigma}(\omega) - A_{2\sigma}(\omega)\right) \\
&\quad + U\left[\langle n_{d\bar{\sigma}}\rangle\left(1 - \langle n_{d\bar{\sigma}}\rangle\right) - \langle d_{\bar{\sigma}} d_\sigma\rangle\langle d_\sigma^\dagger d_{\bar{\sigma}}^\dagger\rangle\right] \\
&\quad - 2i\Gamma_0\langle n_{d\bar{\sigma}}\rangle - \left(B_{1\sigma}(\omega) + B_{2\sigma}(\omega)\right), \\
R_\sigma(\omega) &= \omega - \varepsilon_d - \Sigma_{11}^0(\omega) - U\langle n_{d\bar{\sigma}}\rangle \\
&\quad - \frac{\left(\Sigma_{12}^0(\omega) + U\langle d_{\bar{\sigma}} d_\sigma\rangle\right)\left(\Sigma_{21}^0(\omega) + U\langle d_\sigma^\dagger d_{\bar{\sigma}}^\dagger\rangle\right)}{\omega + \varepsilon_d - \Sigma_{22}^0(\omega) + U\langle n_{d\sigma}\rangle}, \\
T_\sigma(\omega) &= \left(2\varepsilon_d + U\left(1 + \langle n_{d\sigma}\rangle - \langle n_{d\bar{\sigma}}\rangle\right)\right) \\
&\quad \times \langle d_{\bar{\sigma}} d_\sigma\rangle \frac{\Sigma_{21}^0(\omega) + U\langle d_\sigma^\dagger d_{\bar{\sigma}}^\dagger\rangle}{\omega + \varepsilon_d - \Sigma_{22}^0(\omega) + U\langle n_{d\sigma}\rangle},
\end{aligned}
\tag{13}
$$

and the (21)-component of $\widehat{G}_{d\sigma}^r$ is given by

$$
\left[\widehat{G}_{d\sigma}^r(\omega)\right]_{21} = \frac{\Sigma_{21}^0(\omega) + U\langle d_\sigma^\dagger d_{\bar{\sigma}}^\dagger\rangle}{\omega + \varepsilon_d - \Sigma_{22}^0(\omega) + U\langle n_{d\sigma}\rangle}\left[\widehat{G}_{d\sigma}^r(\omega)\right]_{11}. \tag{14}
$$

We can obtain $[\widehat{G}_{d\sigma}^r(\omega)]_{12}$ and $[\widehat{G}_{d\sigma}^r(\omega)]_{22}$ in a similar way, and the final expressions are given in Appendix.

2.2. Current and Electron Occupation Number in the QD. The current from the lead L to the lead R is given by the time derivative of the electron occupation number in the lead L. Applying the equation of motion [37, 38] and the definition $N_L = \sum_{k,\sigma} c_{L,k,\sigma}^\dagger c_{L,k,\sigma}$, we obtain the current I_L as follows [39]:

$$
\begin{aligned}
I_L &= -e\left\langle \frac{dN_L}{dt}\right\rangle = \frac{ie}{\hbar}\left\langle [N_L, H]\right\rangle \\
&= \frac{ie}{\hbar} t \sum_{k,\sigma}\left(\langle c_{L,k,\sigma}^\dagger d_\sigma\rangle - \langle d_\sigma^\dagger c_{L,k,\sigma}\rangle\right) \\
&= \frac{e}{\hbar} t \sum_{k,\sigma}\left(G_{d\sigma,Lk\sigma}^<(t,t) - G_{Lk\sigma,d\sigma}^<(t,t)\right),
\end{aligned}
\tag{15}
$$

where the matrix elements of the lesser Green's functions are denoted as follows: $G_{d\sigma,Lk\sigma}^<(t,t') = i\langle c_{L,k,\sigma}^\dagger(t') d_\sigma(t)\rangle$. Similarly, I_R, which is the current from the lead R to the lead L, is obtained. Using the 2×2 matrix Green's functions and their Fourier-transformed forms, we obtain the Josephson current I as

$$
\begin{aligned}
I &= \frac{1}{2}\left(I_L - I_R\right) \\
&= \frac{1}{2}\frac{et}{2\pi\hbar}\sum_{k,\sigma}\int d\omega \left[\widehat{G}_{d\sigma,Lk\sigma}^<(\omega) - \widehat{G}_{Lk\sigma,d\sigma}^<(\omega)\right. \\
&\quad \left. - \widehat{G}_{d\sigma,Rk\sigma}^<(\omega) + \widehat{G}_{Rk\sigma,d\sigma}^<(\omega)\right]_{11},
\end{aligned}
\tag{16}
$$

where $[\widehat{G}]_{ij}$ is the i,j-th element of $\widehat{G}$. The occupation number of an electron with spin σ in the QD is given by

$$
\begin{aligned}
\langle n_{d\uparrow}\rangle &= \frac{1}{2\pi i}\int d\omega \left[\widehat{G}_{d\uparrow}^<(\omega)\right]_{11}, \\
\langle n_{d\downarrow}\rangle &= \frac{1}{2\pi i}\int d\omega \left[\widehat{G}_{d\downarrow}^<(\omega)\right]_{11}.
\end{aligned}
\tag{17}
$$

The averaged occupation number in the QD is $\langle n_d\rangle = \langle n_{d\uparrow}\rangle + \langle n_{d\downarrow}\rangle$.

To calculate the current (16), the retarded and lesser Green's functions between the QD and the leads are necessary. We can derive these retarded Green's functions by employing the equation of motion, as follows:

$$
\begin{aligned}
\widehat{G}_{d\alpha}^r &= \widehat{G}_{d\sigma}^r \widehat{T} \widehat{g}_{\alpha,\sigma}^r, \\
\widehat{G}_{\alpha d}^r &= \widehat{g}_{\alpha,\sigma}^r \widehat{T} \widehat{G}_{d\sigma}^r.
\end{aligned}
\tag{18}
$$

In the above expressions, we used a simple notation for summation over a wave vector k: $\sum_{k,k'} \widehat{G}_{\alpha k,\beta k'} \equiv \widehat{G}_{\alpha\beta}$. The Langreth theorem states that the lesser Green's function of a matrix $\widehat{A}\widehat{B}$ is given as $[\widehat{A}\widehat{B}]^< = \widehat{A}^r\widehat{B}^< + \widehat{A}^<\widehat{B}^a$ [40]. For equilibrium, by employing the fluctuation dissipation theorem, we obtain $\widehat{G}^<(\omega) = f(\omega)(\widehat{G}^a(\omega) - \widehat{G}^r(\omega))$, where $f(\omega)$ denotes the Fermi distribution function. This function is given as $f(\omega) = 1/(e^{\omega\beta_0} + 1)$ with $\beta_0 = 1/k_B T$, and the Fermi energy is set as $\omega_F = 0$. The advanced Green's function, $G_{ij}^a(\omega)$, is calculated by using the retarded Green's function as $\widehat{G}_{ij}^a(\omega) = (\widehat{G}_{ji}^r(\omega))^\dagger$. Thus, we can construct all Green's functions on the basis of $\widehat{G}_{d\sigma}^r(\omega)$.

The Josephson current consists of two components: the current due to the continuous spectrum for $|\omega| > \Delta$ and that due to the discrete spectrum for $|\omega| < \Delta$:

$$
\begin{aligned}
I &= I_{\text{dis}} + I_{\text{con}}, \\
I_{\text{dis}} &= \frac{e}{2\pi\hbar}\int_{-\Delta}^{\Delta} d\omega f(\omega) j_d(\omega), \\
I_{\text{con}} &= \frac{e}{2\pi\hbar}\left(\int_{-\infty}^{-\Delta} + \int_{\Delta}^{\infty}\right) d\omega f(\omega) j_c(\omega),
\end{aligned}
\tag{19}
$$

where $j_{d(c)}(\omega)$ denotes the discrete (continuous) current density. Under the HF approximation, using the definitions of $\widehat{\Sigma}^0$ and $\widehat{\Sigma}_{d\sigma}^{\text{HF}}$ given in equations (11) and (A.10), respectively, we find that $\widehat{G}_{d\sigma}^r(\omega)$ has singular points (poles). We write the determinant of $(\widehat{G}_{d\sigma}^r(\omega))^{-1}$ as $D(\omega)$, which becomes

$$D(\omega;\varepsilon_d,\theta_L,\theta_R) = \det\left[\left(\widehat{G}^r_{d\sigma}(\omega)\right)^{-1}\right] = ad - bc, \tag{20}$$

where

$$\begin{aligned} a &= \omega - \varepsilon_d + 2i\Gamma_0\rho(\omega) - U\langle n_{d\overline{\sigma}}\rangle, \\ b &= -\sigma i\Gamma_0(\Delta_L + \Delta_R)\rho_0(\omega) - U\langle d_{\overline{\sigma}} d_\sigma\rangle, \\ c &= -\sigma i\Gamma_0(\overline{\Delta}_L + \overline{\Delta}_R)\rho_0(\omega) - U\langle d^\dagger_\sigma d^\dagger_{\overline{\sigma}}\rangle, \\ d &= \omega + \varepsilon_d + 2i\Gamma_0\rho(\omega) + U\langle n_{d\sigma}\rangle, \end{aligned} \tag{21}$$

where $\rho_0(\omega) = \rho(\omega)/\omega$. In our previous study [27], we considered the spin-flip effects on the current in an S/QD/S junction with a Josephson junction in the range $|\omega| < \Delta$. For the system, the HF approximation was applied by neglecting the pairing correlation functions $\langle d^\dagger_\sigma d^\dagger_{\overline{\sigma}}\rangle$ and $\langle d_{\overline{\sigma}} d_\sigma\rangle$. In the absence of direct tunneling between leads and spin-flip effects in the QD, $D(\omega;\varepsilon_d,\theta) = \det[(\widehat{G}^r_{dd}(\omega))^{-1}]$ in that paper coincides with equation (20) without pairing correlation functions. $D(\omega)$ given by equation (20) is a quadratic function in terms of ω, and consequently, two poles can occur in $\widehat{G}^r_{d\sigma}(\omega)$. When $\rho(\omega)$ is given, $D(\omega)$ has a finite imaginary part for $|\omega| > \Delta$. On the contrary, $D(\omega)$ has a real part with an infinitesimal imaginary part for $|\omega| < \Delta$. The ABSs exist inside the gap $|\omega| < \Delta$, and their positions correspond to the poles of Green's function $\widehat{G}^r_{d\sigma}(\omega)$. The discrete current I_{dis} originates from the ABSs, and to calculate I_{dis}, we employ the Sokhotski–Plemelj formula, $\lim_{\omega\longrightarrow\omega_0}\int d\omega/g(\omega) = -i\pi/g'(\omega_0)$, where ω_0 is a real solution of $g(\omega_0) = 0$ denoting the position of the ABS. On the contrary, the continuous spectrum outside the gap $|\omega| > \Delta$ contributes to the continuous current I_{con}, which is calculated by means of the usual numerical integral.

In this study, we consider the system to be at zero temperature, and all the energy quantities are scaled by the BCS gap Δ. Without loss of generality, we put $\theta_R = -\theta_L$, and the BCS phase difference between the left and right superconducting leads is set as $\theta = \theta_L - \theta_R$. We set the DOS in the leads in the normal state $\nu = 1/(2W)$ in the range $|\omega| \le W$, where we choose the half bandwidth $W = 20$ such that W is much larger than all other energy scales.

3. Numerical Calculation Results

Here, we show the numerical calculation results obtained by the Lacroix approximation. We define the total density of states in the QD as $\rho_d(\omega) = -(1/\pi)\sum_\sigma \mathrm{Im}[\widehat{G}^r_{d\sigma}(\omega)]_{11}$, and ρ_d is shown in Figure 2. In our calculation, the multiple integral over ω is divided into two regions: $|\omega| > \Delta$ and $|\omega| < \Delta$. $\rho(\omega)$ defined by equation (6) diverges at $|\omega| = \Delta$; therefore, a sharp peak and dip are observed around $|\omega| = 1$ in ρ_d. In the case of the particle-hole symmetric case, $\varepsilon_d = -U/2$, we observe the Coulomb peaks around $\omega = \pm U/2$ (Figure 2(a)). However, it is known that the Kondo peak at the Fermi level ($\omega = 0$) does not appear in the Lacroix approximation. On the contrary, in the case of the particle-hole asymmetric case, we observe the Coulomb peaks around $\omega = \varepsilon_d$ and $\varepsilon_d + U$, and the antiresonant dip is observed around $\omega = U + 2\varepsilon_d$ (Figure 2(b)). This unphysical resonance is a specific characteristic of the Lacroix approximation, which disappears in the limit $U \longrightarrow \infty$ [29, 41]. In Figure 2(c), the Kondo peak is observed around the Fermi level.

The dependence of the current on the BCS phase difference is shown in Figure 3. In the case of the HF approximation, the current I is expressed in the form $I = I_c \sin\theta$, where I_c is called the critical current and θ is the BCS phase difference. In the HF approximation, the amplitude I_c depends slightly on θ, and the phase shift occurs when ε_d is chosen in the range $-U < \varepsilon_d < 0$ (Figure 3(a)). That is, the current-phase relations change from $I = |I_c|\sin\theta$ to $I = -|I_c|\sin\theta$ with changing ε_d, which is called the 0-π transition [42]. A similar property is observed in the Lacroix approximation (Figure 3(b)). However, a difference is that the current amplitude I_c depends strongly on the phase θ. This is caused by different calculation schemes employed by the two approximations; the HF approximation is a type of mean-field theory, taking only the nonconnected part in $\widehat{F}_{d\sigma}$ into consideration, and the macroscopic parameters $\langle n_{d\sigma}\rangle$ and $\langle d^\dagger_\sigma d^\dagger_{\overline{\sigma}}\rangle$ are determined self-consistently. On the contrary, in the Lacroix approximation, by taking the connected term $\widehat{F}^c_{d\sigma}$ into consideration, these macroscopic parameters are self-consistently determined for each θ. As a result, these parameters are dependent on θ. Although the current satisfies $I = 0$ at $\theta = 0, \pm\pi$, it deviates from the relation $I = I_c \sin\theta$ with a fixed I_c.

Let us consider the 0-π transition in terms of the Kondo temperature and the BCS gap under a large Coulomb repulsion. The Kondo temperature T_{K} in the normal conductor connected to a QD is given by several calculation schemes. T_{K} calculated by scaling theory is $T_{\mathrm{K}} = \Gamma\sqrt{U/(2\Gamma)}\exp[\pi\varepsilon_d(1 + \varepsilon_d/U)/(2\Gamma)]$, where $\Gamma = 2\pi\nu t^2$ [43]. For the SU(N) Anderson impurity model, T_{K} calculated by the renormalization group scaling theory is $T_{\mathrm{K}} = \exp[\pi\varepsilon_d/(N\Gamma)]$ [44]. However, for the same model, T_{K} calculated by the Lacroix approximation is $T_{\mathrm{K}} = W\exp[\pi\varepsilon_d/((N-1)\Gamma)]$ [29, 45]. Although the formulation by the Lacroix truncation scheme is rather crude, it can qualitatively capture the 0-π transition in the S/QD/S system, where the Kondo effect and superconductivity compete against each other [35]. The relative magnitude of Δ and T_{K} determines the characteristics of the dependence of the current on the BCS phase difference. In the weak coupling case, $\Delta \gg T_{\mathrm{K}}$, the π-junction is observed, and the ground state of the QD is doublet (dashed curve in Figure 3(b)). On the contrary, in the strong coupling case, $T_{\mathrm{K}} \gg \Delta$, the 0-junction is observed, and the ground state of the QD is the Kondo singlet (solid curve in Figure 3(b)). Comparing the results obtained by our Lacroix approximation with those obtained by the HF approximation (Figure 3(a)), the dependence of the current on the BCS phase difference θ is highly nonsinusoidal. For the intermediate coupling case, $T_{\mathrm{K}} \sim \Delta$, and the dependence of the current breaks into three different regions. In the central region around $\theta = 0$, the behavior of the current resembles that in the ballistic short junction: the current changes linearly with θ. In the surrounding two regions,

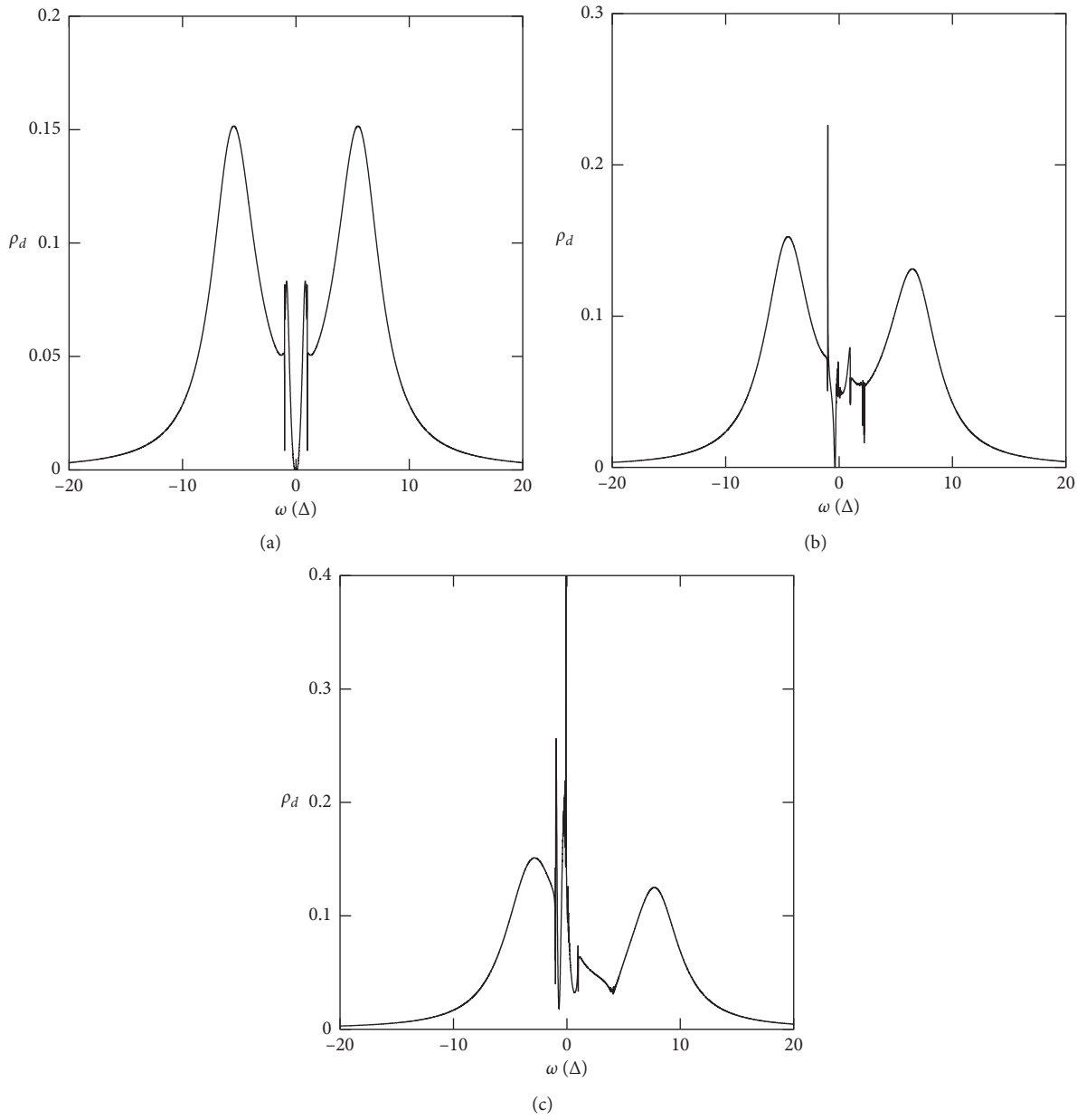

Figure 2: Total local density of states in the QD for $\Gamma_0 = 0.5$ and $U = 12$. (a) $\varepsilon_d = -6$. (b) $\varepsilon_d = -5$. (c) $\varepsilon_d = -4$.

the dependence of the current on the phase is similar to that in a π-junction (Figure 3(c)). At the transition point $T_K \sim \Delta$, we obtain $\varepsilon_d \sim [(N-1)\Gamma \ln(\Delta/W)]/\pi$ by using the Lacroix expression. In our parameters with $N = 2$, $\varepsilon_d \sim -0.2$. This value does not agree with our numerical calculation result, $\varepsilon_d \sim -5.5$. In spite of this discrepancy, the above-mentioned properties of dependence of current on the BCS phase difference are qualitatively consistent with the results obtained by the NRG method [13]. In our calculation of HF approximation, a complex dependence of the current on the phase, such as that in Figure 3(c), did not occur around the transition point $T_K \sim \Delta$.

The dependence of the averaged occupation number of the electrons in the QD on the QD energy level is shown in Figure 4. For a much smaller ε_d such as $\varepsilon_d \ll -U$, $\langle n_d \rangle \sim 2$. Intermediate values of ε_d such as $-U < \varepsilon_d < 0$, where $\langle n_d \rangle \sim 1$, define a magnetic region in which a π-junction occurs. For larger values of ε_d satisfying $\varepsilon_d > 0$, $\langle n_d \rangle \sim 0$. This property is identical for both the HF and the Lacroix approximations.

The current density distribution under the HF approximation is shown in Figure 5(a). The total current density is defined as $j(\omega) = j_d(\omega) + j_c(\omega)$. When ε_d is chosen such that $\varepsilon_d \sim -U$, we can find sharp peaks within the BCS gap Δ in the current density distribution j. The positions of these peaks correspond to the zero of D. There is an ABS below the Fermi level, and it carries a negative current. Although $j_c > 0$, it is generally small and satisfies $j_c \ll |j_d|$ so that $j < 0$ (π-junction) [46]. The dependence of the pole positions of Green's function $[\widehat{G}^r_{d\sigma}(\omega)]_{11}$ on ε_d is shown in Figure 5(b). We defined $\omega^0_{\pm}$ as the real solutions

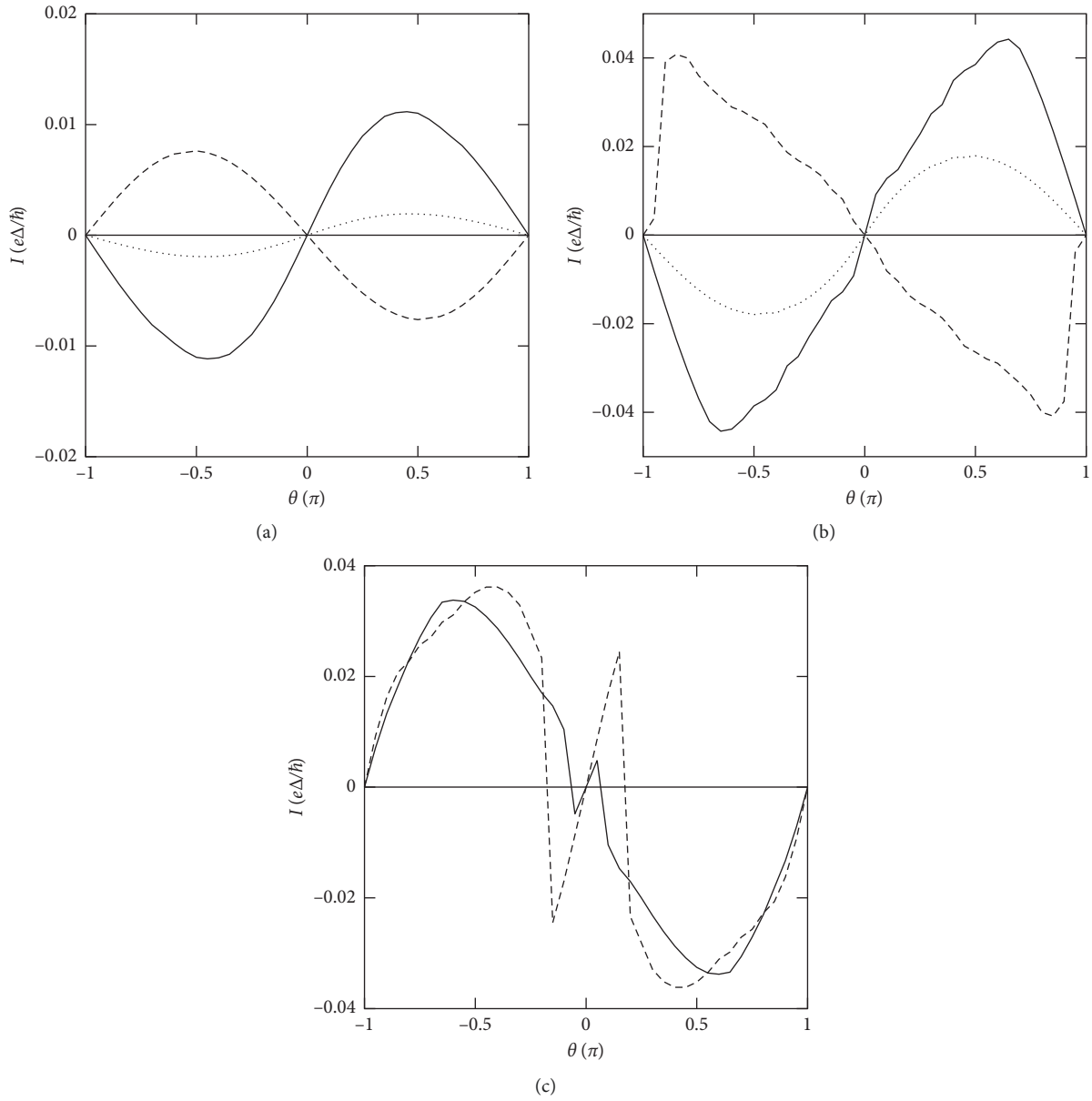

Figure 3: Dependence of the current on the BCS phase difference for $\Gamma_0 = 0.1$ and $U = 5$. (a) HF approximation: the solid, dashed, and dotted curves correspond to cases $\varepsilon_d = 1$, -3, and -7, respectively. (b) Lacroix approximation: the solid, dashed, and dotted curves correspond to cases $\varepsilon_d = 0$, -4, and -7.5, respectively. (c) Lacroix approximation: the solid and dashed curves correspond to cases $\varepsilon_d = -5.5$ and -6.0, respectively.

of $D(\omega) = 0$ within the BCS gap, $|\omega_{\pm}^0| < \Delta$. Here, $\omega_{\pm}^0$ corresponds to the position of the ABS, and we find that $\omega_{-}^0 \simeq -\omega_{+}^0$ is satisfied [47]. On the contrary, in the Lacroix approximation, $[\widehat{G}_{d\sigma}^r(\omega)]_{11}$ is given by equation (12), which is described by the variables P_σ, Q_σ, R_σ, and T_σ. If P_σ, Q_σ, and T_σ are neglected, $[\widehat{G}_{d\sigma}^r(\omega)]_{11} = 1/R_\sigma(\omega)$, which agrees with the result obtained from the HF approximation [27]. When the connected term $\widehat{F}_{d\sigma}^c$ is considered, P_σ, Q_σ, and T_σ appear in the expression of $[\widehat{G}_{d\sigma}^r(\omega)]_{11}$. We see that P_σ and Q_σ have finite imaginary parts due to the terms proportional to $i\Gamma_0$, and R_σ and T_σ have a similar property: for $|\omega| > \Delta$, R_σ and T_σ have finite imaginary parts. On the contrary, for $|\omega| < \Delta$, R_σ and T_σ have real parts with an infinitesimal imaginary part. In our Lacroix approximation, we define $D(\omega)$ as $D = P_\sigma R_\sigma - U(Q_\sigma + T_\sigma)$. Then, unlike the HF approximation, D has a finite imaginary part for any value of ω, and there is no real solution for $D = 0$ in the range $|\omega| < \Delta$.

The dependence of the critical current on the QD energy level is shown in Figure 6. In the case $U = 0$, I_c is positive, and it diverges at $\varepsilon_d = 0$ (Figure 6(a)). For a finite U, we apply the HF or Lacroix approximations. Generally, for $U < \Gamma_0$, $n_{d\uparrow}$ and $n_{d\downarrow}$ are almost equal, and the current is positive with a maximum at $\varepsilon_d = -U/2$. By contrast, for $U > \Gamma_0$, $n_{d\uparrow}$ and $n_{d\downarrow}$

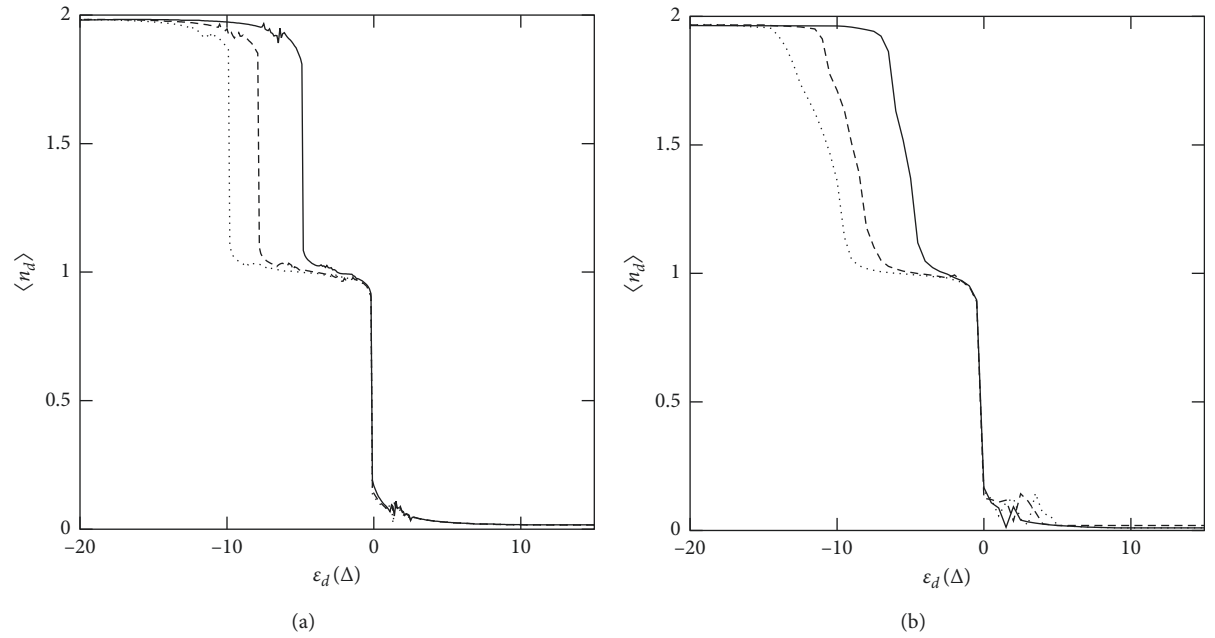

FIGURE 4: Dependence of the averaged occupation number in the QD on the QD energy level for $\Gamma_0 = 0.1$ and $\theta = \pi/2$. The solid, dashed, and dotted curves correspond to cases $U = 5$, 8, and 10, respectively. (a) HF approximation. (b) Lacroix approximation.

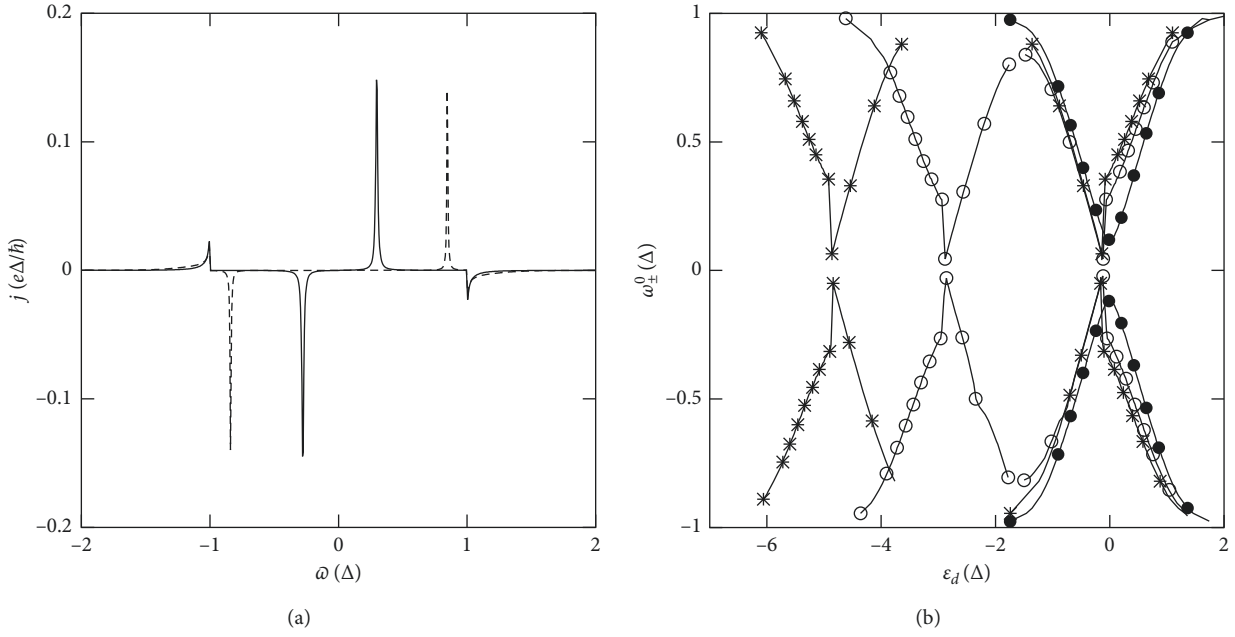

FIGURE 5: Current density and dependence of the pole position on the QD energy level. The data are obtained by the HF approximation for $\Gamma_0 = 0.1$ and $\theta = \pi/2$. (a) Current density. The solid and dashed curves correspond to cases $U = 3$ with $\varepsilon_d = -3$ and $\varepsilon_d = -4$, respectively. (b) Dependence of the pole positions of $\widehat{G}^{(0)r}_{d\sigma}$ on the QD energy level. The solid curves with symbols •, ◦, and ∗ correspond to cases $U = 0$, 3, and 5, respectively.

are not equal, and therefore, the QD becomes magnetic. In the HF approximation, the π-junction occurs in the range $-U < \varepsilon_d < 0$ (Figure 6(b)). By contrast, in our Lacroix approximation, although the π-junction occurs around $\varepsilon_d \sim -U$ or 0, it does not occur in the entire range $-U < \varepsilon_d < 0$ (Figure 6(c)). Current I is composed of I_{dis} and I_{con}, and the dependence of I_{dis} and I_{con} on ε_d is shown in Figure 6(d). Because there is no real solution for $D = 0$, I_{dis} and I_{con} were calculated by the usual integral. We see that I_{dis} and I_{con} have similar properties; I_{dis} and I_{con} are negative around $\varepsilon_d \sim -U$ and Δ, but I_{dis} and I_{con} are positive with a sharp peak around $\varepsilon_d \sim -(U + \Delta)$ and 0. Thus, in our calculations, even if there is

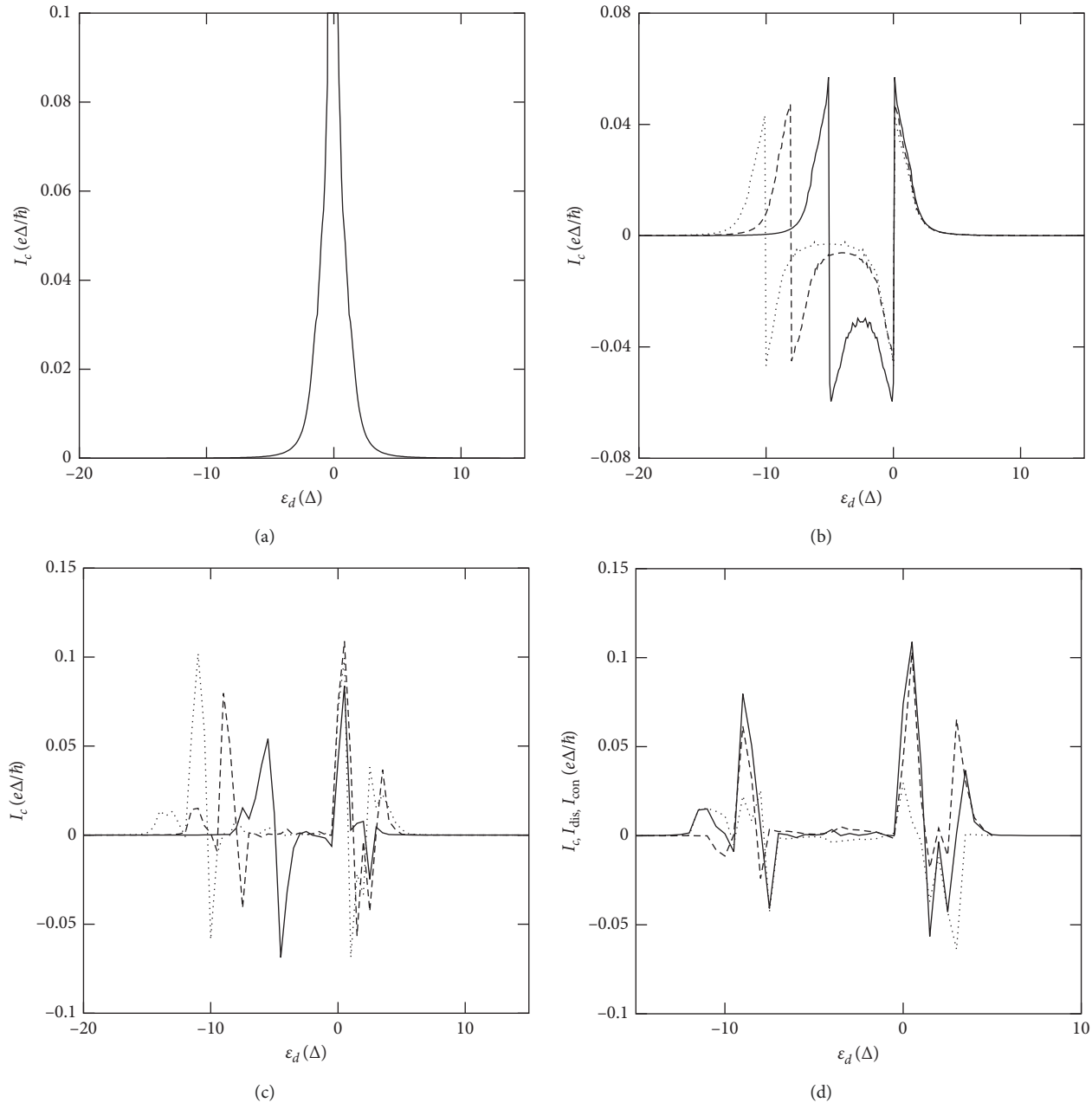

FIGURE 6: Dependence of the critical current on the QD energy level for $\Gamma_0 = 0.1$ and $\theta = \pi/2$. (a) $U = 0$. (b) HF approximation. (c) Lacroix approximation. The solid, dashed, and dotted curves correspond to cases $U = 5$, 8, and 10, respectively. (d) Component of I_c. $U = 8$ and the data are obtained by the Lacroix approximation. The solid, dashed, and dotted curves represent I_c, I_{dis}, and I_{con}, respectively.

no real solution for $D = 0$ in the range $-U < \varepsilon_d < 0$, a negative current (critical current $I_c < 0$) occurs around $\varepsilon_d \sim -U$ and Δ.

4. Conclusions

We have studied the current in an S/QD/S junction system with Coulomb interaction. In the HF approximation, up to the first order of tunneling amplitude t was considered, while the electron correlation was not considered sufficiently; therefore, it was necessary to include a higher-order Green's function. In this study, the Lacroix approximation was applied, where up to the second order of t was considered. In the HF approximation, the connected term $\widehat{F}^c_{d\sigma}$ was neglected in the cluster expansion, and the macroscopic parameters $\langle n_{d\sigma}\rangle$, $\langle d^\dagger_\sigma d^\dagger_{\bar\sigma}\rangle$, and $\langle d_{\bar\sigma} d_\sigma\rangle$ were self-consistently determined. It turned out that this simplification corresponded to the neglect of $\langle\langle d_\sigma n_{d\bar\sigma}; d^\dagger_\sigma\rangle\rangle_c$, $\langle\langle c_{\alpha,k,\sigma} n_{d\bar\sigma}; d^\dagger_\sigma\rangle\rangle_c$, $\langle\langle d^\dagger_{\bar\sigma} c_{\alpha,k,\bar\sigma} d_\sigma; d^\dagger_\sigma\rangle\rangle_c$, and $\langle\langle c^\dagger_{\alpha,k,\bar\sigma} d_{\bar\sigma} d_\sigma;\ d^\dagger_\sigma\rangle\rangle_c$ in the expansion of the higher-order Green's functions. The lack of these connected terms is a crucial defect when we consider low-temperature physics such as Kondo physics. In our Lacroix approximation, the connected term $\widehat{F}^c_{d\sigma}$ was taken into consideration under several simplifications; the superconducting correlation functions involved in the QD and leads and all the pairing

corrections obtained from higher-order Green's functions were neglected. Under these simplifications, we calculated $\langle\langle d_\sigma; d_\sigma^\dagger\rangle\rangle$ and $\langle\langle d_{\overline{\sigma}}^\dagger; d_{\overline{\sigma}}\rangle\rangle$ self-consistently.

In our Lacroix approximation, $\langle\langle d_\sigma; d_\sigma^\dagger\rangle\rangle$ was expressed by the variables P_σ, Q_σ, R_σ, and T_σ. When the connected term $\widehat{F}_{d\sigma}^c$ was not considered, P_σ, Q_σ, and T_σ vanished, giving $\langle\langle d_\sigma; d_\sigma^\dagger\rangle\rangle = 1/R_\sigma$, which recovered the expression obtained by the HF approximation [27]. The denominator of $\langle\langle d_\sigma; d_\sigma^\dagger\rangle\rangle$ was defined as $D(\omega)$. In the HF approximation, when we chose $\varepsilon_d \sim -U$ or 0 for a finite U, there were two real solutions for $D = 0$ in the range $|\omega| < \Delta$. One solution below the Fermi level yielded a negative current, and the π-junction occurred in the range $-U < \varepsilon_d < 0$. On the contrary, in our Lacroix approximation, there was no real solution for $D = 0$, which results from our calculation scheme based on the Lacroix approximation; the variables P_σ and Q_σ were complex for the entire range of ω because of the terms proportional to $i\Gamma_0$. As a result, although the π-junction did not occur in the entire range $-U < \varepsilon_d < 0$, the negative current occurred only around $\varepsilon_d \sim -U$ and Δ.

In the HF approximation, the higher-order electron correlation is inherently not taken into consideration, and therefore, a discussion of the characteristics of the current in terms of the ratio Δ/T_K is inappropriate. Although higher-order Green's functions are taken into consideration under simplifications in the Lacroix approximation, it is not a precise calculation compared with the NRG, functional RG, and QMC methods [48]. In fact, our numerical calculation results did not agree well with T_K estimated by Lacroix. In spite of this discrepancy, our numerical calculation results captured several aspects of the 0-π transition and the Kondo resonance in restricted parameters. However, our Lacroix approximation could not capture well the competition between Kondo physics and π-junction for all the parameters. The Lacroix approximation employs a truncation at the second order of t and applies cluster expansion for higher-order Green's functions. Under these simplifications, reliable calculation results are obtained in restricted parameters, and only the qualitative features of Kondo physics in superconductors are obtained.

Appendix

A. Derivation of Green's Function of the QD

In this section, we present the derivation of $\widehat{G}_{d\sigma}^r(\omega)$ following reference [49], in which the normal conductor/QD/S junction was considered. We use the Zubarev notation for the retarded Green's function, $G_{A,B}^r(\omega) = \langle\langle A; B\rangle\rangle$, which is composed of the operators A and B. The equation of motion of $\langle\langle A; B\rangle\rangle$ is given by

$$\omega\langle\langle A; B\rangle\rangle = \langle [A, B]_+\rangle + \langle\langle [A, H]_-; B\rangle\rangle, \tag{A.1}$$

where $[A, B]_\pm = AB \pm BA$. We first derive the equations of motion of each element of the retarded Green's function $\widehat{G}_{d\sigma}^r(\omega)$ given by equation (7):

$$\begin{aligned}&(\omega - \varepsilon_d - \Gamma_1(\omega))\langle\langle d_\sigma; d_\sigma^\dagger\rangle\rangle + \Lambda_1\langle\langle d_{\overline{\sigma}}^\dagger; d_\sigma^\dagger\rangle\rangle \\ &\quad = 1 + U\langle\langle d_\sigma n_{d\overline{\sigma}}; d_\sigma^\dagger\rangle\rangle,\end{aligned} \tag{A.2}$$

$$\begin{aligned}&(\omega + \varepsilon_d - \Gamma_2(\omega))\langle\langle d_{\overline{\sigma}}^\dagger; d_\sigma^\dagger\rangle\rangle - \Lambda_2\langle\langle d_\sigma; d_\sigma^\dagger\rangle\rangle \\ &\quad = -U\langle\langle d_{\overline{\sigma}}^\dagger n_{d\sigma}; d_\sigma^\dagger\rangle\rangle,\end{aligned} \tag{A.3}$$

$$\begin{aligned}&(\omega - \varepsilon_d - \Gamma_1(\omega))\langle\langle d_\sigma; d_{\overline{\sigma}}\rangle\rangle + \Lambda_1\langle\langle d_{\overline{\sigma}}^\dagger; d_{\overline{\sigma}}\rangle\rangle \\ &\quad = U\langle\langle d_\sigma n_{d\overline{\sigma}}; d_{\overline{\sigma}}\rangle\rangle,\end{aligned} \tag{A.4}$$

$$\begin{aligned}&(\omega + \varepsilon_d - \Gamma_2(\omega))\langle\langle d_{\overline{\sigma}}^\dagger; d_{\overline{\sigma}}\rangle\rangle - \Lambda_2\langle\langle d_\sigma; d_{\overline{\sigma}}\rangle\rangle \\ &\quad = 1 - U\langle\langle d_{\overline{\sigma}}^\dagger n_{d\sigma}; d_{\overline{\sigma}}\rangle\rangle,\end{aligned} \tag{A.5}$$

where we put $\Gamma_1(\omega) = \sum_{k,\alpha} t^2(\omega + \varepsilon_k)/E_k^2$, $\Gamma_2(\omega) = \sum_{k,\alpha} t^2(\omega - \varepsilon_k)/E_k^2$, $\Lambda_1(\omega) = \sum_{k,\alpha} \sigma\Delta_\alpha(t^2/E_k^2)$, and $\Lambda_2(\omega) = \sum_{k,\alpha} \overline{\sigma}\overline{\Delta}_\alpha(t^2/E_k^2)$ with $E_k^2 = \omega^2 - \varepsilon_k^2 - \Delta^2$. For the symbols $\sigma = \uparrow, \downarrow$, + and − are, respectively, assigned for the up- and downspins in the mathematical calculations. Replacing the sum over the wavenumber k by an integral, we obtain $\Gamma_1(\omega) = \Gamma_2(\omega) = -2i\Gamma_0\rho(\omega)$, $\Lambda_1 = -i\Gamma_0\sigma(\Delta_L + \Delta_R)\rho_0(\omega)$, and $\Lambda_2 = -i\Gamma_0\overline{\sigma}(\overline{\Delta}_L + \overline{\Delta}_R)\rho_0(\omega)$, where $\Gamma_0 = \pi\nu t^2$, $\rho(\omega) = (|\omega|\theta(|\omega| - \Delta)/\sqrt{\omega^2 - \Delta^2}) + (\omega\theta(\Delta - |\omega|)/i\sqrt{\Delta^2 - \omega^2})$, and $\rho_0(\omega) = (\mathrm{sgn}(\omega)\theta(|\omega| - \Delta)/\sqrt{\omega^2 - \Delta^2}) + (\theta(\Delta - |\omega|)/i\sqrt{\Delta^2 - \omega^2})$. Here, $\theta(\omega)$ and $\mathrm{sgn}(\omega)$ are the Heaviside step function and the sign function, respectively.

To simplify the description of equations (A.2)–(A.5), we introduce a matrix $\widehat{F}_{d\sigma}(\omega)$ as

$$\widehat{F}_{d\sigma}(\omega) = \begin{pmatrix} \langle\langle d_\sigma n_{d\overline{\sigma}}; d_\sigma^\dagger\rangle\rangle & \langle\langle d_\sigma n_{d\overline{\sigma}}; d_{\overline{\sigma}}\rangle\rangle \\ -\langle\langle d_{\overline{\sigma}}^\dagger n_{d\sigma}; d_\sigma^\dagger\rangle\rangle & -\langle\langle d_{\overline{\sigma}}^\dagger n_{d\sigma}; d_{\overline{\sigma}}\rangle\rangle \end{pmatrix}. \tag{A.6}$$

Using these expressions, equations (A.2)–(A.5) are written in the matrix form as

$$\left[\widehat{G}_{d\sigma}^{(0)r}(\omega)\right]^{-1}\widehat{G}_{d\sigma}^r(\omega) = \widehat{I} + U\widehat{F}_{d\sigma}(\omega), \tag{A.7}$$

where $\widehat{I}$ is an identity matrix and

$$\left[\widehat{G}_{d\sigma}^{(0)r}(\omega)\right]^{-1} = \begin{pmatrix} \omega - \varepsilon_d - \Sigma_{11}^0(\omega) & -\Sigma_{12}^0(\omega) \\ -\Sigma_{21}^0(\omega) & \omega + \varepsilon_d - \Sigma_{22}^0(\omega) \end{pmatrix}, \tag{A.8}$$

where $\widehat{\Sigma}^0$ is a noninteracting self-energy with components $\Sigma_{11}^0 = \Sigma_{22}^0 = -i(\Gamma_L^0 + \Gamma_R^0)\rho(\omega) \equiv -2i\Gamma_0\rho(\omega)$, $\Sigma_{12}^0 = \sigma i\Gamma_0(\Delta_L + \Delta_R)\rho_0(\omega)$, and $\Sigma_{21}^0 = \sigma i\Gamma_0(\overline{\Delta}_L + \overline{\Delta}_R)\rho_0(\omega)$, where we used the property $\Gamma_L^0 = \Gamma_R^0 \equiv \Gamma_0$. It is known that equation (A.6) is not closed because $\widehat{F}_{d\sigma}$ includes the higher-order terms of $\widehat{G}_{d\sigma}$. To overcome this difficulty, we employ the truncation approximation. We first expand $\widehat{F}_{d\sigma}$ as

$$\widehat{F}_{d\sigma} = \widehat{\Sigma}_{d\sigma}^{HF}\widehat{G}_{d\sigma}^r(\omega) + \widehat{F}_{d\sigma}^c(\omega), \tag{A.9}$$

where $\widehat{\Sigma}_{d\sigma}^{\mathrm{HF}}$ is the nonconnected part, which is given as

$$\widehat{\Sigma}^{HF}_{d\sigma} = \begin{pmatrix} \langle n_{d\overline{\sigma}}\rangle & \langle d_{\overline{\sigma}} d_{\sigma}\rangle \\ \langle d^{\dagger}_{\sigma} d^{\dagger}_{\overline{\sigma}}\rangle & -\langle n_{d\sigma}\rangle \end{pmatrix}, \tag{A.10}$$

and the connected part is

$$\widehat{F}^{c}_{d\sigma}(\omega) = \begin{pmatrix} \langle\langle d_{\sigma} n_{d\overline{\sigma}}; d^{\dagger}_{\sigma}\rangle\rangle_{c} & \langle\langle d_{\sigma} n_{d\overline{\sigma}}; d_{\overline{\sigma}}\rangle\rangle_{c} \\ -\langle\langle d^{\dagger}_{\overline{\sigma}} n_{d\sigma}; d^{\dagger}_{\sigma}\rangle\rangle_{c} & -\langle\langle d^{\dagger}_{\overline{\sigma}} n_{d\sigma}; d_{\overline{\sigma}}\rangle\rangle_{c} \end{pmatrix}. \tag{A.11}$$

When the connected part is neglected, $\widehat{G}_{d\sigma}$ satisfies the relation

$$\left(\left[\widehat{G}^{(0)r}_{d\sigma}(\omega)\right]^{-1} - U\widehat{\Sigma}^{HF}_{d\sigma}(\omega)\right)\widehat{G}^{r}_{d\sigma}(\omega) = \widehat{I}. \tag{A.12}$$

The solution of (A.12) is obtained self-consistently. The occupation number in the QD $\langle n_{d\sigma}\rangle$ and the pairing correlation function $\langle d^{\dagger}_{\sigma} d^{\dagger}_{\overline{\sigma}}\rangle$ are given by the relations

$$\langle n_{d\sigma}\rangle = -\frac{1}{\pi}\int d\omega\, f(\omega)\mathrm{Im}\left[\widehat{G}^{r}_{d\sigma}(\omega)\right]_{11},$$

$$\langle d^{\dagger}_{\sigma} d^{\dagger}_{\overline{\sigma}}\rangle = \langle d_{\overline{\sigma}} d_{\sigma}\rangle = -\frac{1}{\pi}\int d\omega\, f(\omega)\mathrm{Im}\left[\widehat{G}^{r}_{d\sigma}(\omega)\right]_{21}, \tag{A.13}$$

where $f(\omega)$ is the Fermi distribution function with the Fermi level $\omega_{\mathrm{F}} = 0$.

Beyond the HF approximation, one needs to take $\widehat{F}^{c}_{d\sigma}$ into consideration. For the study of Kondo physics, we need to consider only the contributions from the diagonal components in equation (A.11) [50, 51]. Here, we apply the Lacroix truncation, where the second order of connection $O(t^2)$ is considered. In this approximation, although the diagonal components of $\widehat{F}^{c}_{d\sigma}$ are considered, anomalous higher-order Green's functions such as $\langle\langle d_{\sigma} n_{d\overline{\sigma}}; d_{\overline{\sigma}}\rangle\rangle_{c}$ and $\langle\langle d^{\dagger}_{\overline{\sigma}} n_{d\sigma}; d^{\dagger}_{\sigma}\rangle\rangle_{c}$ are neglected. This yields the relation

$$\langle\langle d^{\dagger}_{\overline{\sigma}}; d^{\dagger}_{\sigma}\rangle\rangle = \frac{\Sigma^{0}_{21}(\omega) + U\langle d^{\dagger}_{\sigma} d^{\dagger}_{\overline{\sigma}}\rangle}{\omega + \varepsilon_{d} - \Sigma^{0}_{22}(\omega) + U\langle n_{d\sigma}\rangle}\langle\langle d_{\sigma}; d^{\dagger}_{\sigma}\rangle\rangle, \tag{A.14}$$

and equation (A.2) becomes

$$\begin{aligned} &\left(\omega - \varepsilon_{d} - \Sigma^{0}_{11}(\omega) - U\langle\langle n_{d\overline{\sigma}}\rangle\rangle\right)\langle\langle d_{\sigma}; d^{\dagger}_{\sigma}\rangle\rangle \\ &\quad -\left(\Sigma^{0}_{12}(\omega) + U\langle d_{\overline{\sigma}} d_{\sigma}\rangle\right)\langle\langle d^{\dagger}_{\overline{\sigma}}; d^{\dagger}_{\sigma}\rangle\rangle \\ &\quad = 1 + U\langle\langle d_{\sigma} n_{d\overline{\sigma}}; d^{\dagger}_{\sigma}\rangle\rangle_{c}. \end{aligned} \tag{A.15}$$

All we have to do is to calculate $\langle\langle d_{\sigma} n_{d\overline{\sigma}}; d^{\dagger}_{\sigma}\rangle\rangle_{c}$ self-consistently. The procedure is as follows. The equation of motion of $\langle\langle d_{\sigma} n_{d\overline{\sigma}}; d^{\dagger}_{\sigma}\rangle\rangle$ is given by

$$\begin{aligned} (\omega - \varepsilon_{d} - U)\langle\langle d_{\sigma} n_{d\overline{\sigma}}; d^{\dagger}_{\sigma}\rangle\rangle &= \langle n_{d\overline{\sigma}}\rangle + \sum_{\alpha,k} t\langle\langle c_{\alpha,k,\sigma} n_{d\overline{\sigma}}; d^{\dagger}_{\sigma}\rangle\rangle \\ &\quad + \sum_{\alpha,k} t\Big(\langle\langle d^{\dagger}_{\overline{\sigma}} c_{\alpha,k,\overline{\sigma}} d_{\sigma}; d^{\dagger}_{\sigma}\rangle\rangle \\ &\quad - \langle\langle c^{\dagger}_{\alpha,k,\overline{\sigma}} d_{\overline{\sigma}} d_{\sigma}; d^{\dagger}_{\sigma}\rangle\rangle\Big). \end{aligned} \tag{A.16}$$

The higher-order Green's functions, $\langle\langle c_{\alpha,k,\sigma} n_{d\overline{\sigma}}; d^{\dagger}_{\sigma}\rangle\rangle$, $\langle\langle d^{\dagger}_{\overline{\sigma}} c_{\alpha,k,\overline{\sigma}} d_{\sigma}; d^{\dagger}_{\sigma}\rangle\rangle$, and $\langle\langle c^{\dagger}_{\alpha,k,\overline{\sigma}} d_{\overline{\sigma}} d_{\sigma}; d^{\dagger}_{\sigma}\rangle\rangle$, are included in the right-hand side of equation (A.16). The equations of motion of these higher-order Green's functions are

$$\begin{aligned} (\omega - \varepsilon_{k})\langle\langle c_{\alpha,k,\sigma} n_{d\overline{\sigma}}; d^{\dagger}_{\sigma}\rangle\rangle &= t\langle\langle d_{\sigma} n_{d\overline{\sigma}}; d^{\dagger}_{\sigma}\rangle\rangle \\ &\quad + \sigma\Delta_{\alpha}\langle\langle c^{\dagger}_{\alpha,-k,\overline{\sigma}} n_{d\overline{\sigma}}; d^{\dagger}_{\sigma}\rangle\rangle \\ &\quad + \sum_{\alpha',k'} t\Big(\langle\langle d^{\dagger}_{\overline{\sigma}} c_{\alpha',k',\overline{\sigma}} c_{\alpha,k,\sigma}; d^{\dagger}_{\sigma}\rangle\rangle \\ &\quad - \langle\langle c^{\dagger}_{\alpha',k',\overline{\sigma}} d_{\overline{\sigma}} c_{\alpha,k,\sigma}; d^{\dagger}_{\sigma}\rangle\rangle\Big), \end{aligned} \tag{A.17}$$

$$\begin{aligned} \left(\omega - \omega_{1,k}\right)\langle\langle d^{\dagger}_{\overline{\sigma}} c_{\alpha,k,\overline{\sigma}} d_{\sigma}; d^{\dagger}_{\sigma}\rangle\rangle &= \langle d^{\dagger}_{\overline{\sigma}} c_{\alpha,k,\overline{\sigma}}\rangle + t\langle\langle d_{\sigma} n_{d\overline{\sigma}}; d^{\dagger}_{\sigma}\rangle\rangle \\ &\quad + \overline{\sigma}\Delta_{\alpha}\langle\langle d^{\dagger}_{\overline{\sigma}} c^{\dagger}_{\alpha,-k,\sigma} d_{\sigma}; d^{\dagger}_{\sigma}\rangle\rangle \\ &\quad + \sum_{\alpha',k'} t\Big(\langle\langle d^{\dagger}_{\overline{\sigma}} c_{\alpha,k,\overline{\sigma}} c_{\alpha',k',\sigma}; d^{\dagger}_{\sigma}\rangle\rangle \\ &\quad - \langle\langle c^{\dagger}_{\alpha',k',\overline{\sigma}} c_{\alpha,k,\overline{\sigma}} d_{\sigma}; d^{\dagger}_{\sigma}\rangle\rangle\Big), \end{aligned} \tag{A.18}$$

$$\begin{aligned} \left(\omega - \omega_{2,k}\right)\langle\langle c^{\dagger}_{\alpha,k,\overline{\sigma}} d_{\overline{\sigma}} d_{\sigma}; d^{\dagger}_{\sigma}\rangle\rangle &= \langle c^{\dagger}_{\alpha,k,\overline{\sigma}} d_{\overline{\sigma}}\rangle - t\langle\langle d_{\sigma} n_{d\overline{\sigma}}; d^{\dagger}_{\sigma}\rangle\rangle \\ &\quad - \overline{\sigma}\Delta_{\alpha}\langle\langle c_{\alpha,-k,\sigma} d_{\overline{\sigma}} d_{\sigma}; d^{\dagger}_{\sigma}\rangle\rangle \\ &\quad + \sum_{\alpha',k'} t\Big(\langle\langle c^{\dagger}_{\alpha,k,\overline{\sigma}} c_{\alpha',k',\overline{\sigma}} d_{\sigma}; d^{\dagger}_{\sigma}\rangle\rangle \\ &\quad + \langle\langle c^{\dagger}_{\alpha,k,\overline{\sigma}} d_{\overline{\sigma}} c_{\alpha',k',\sigma}; d^{\dagger}_{\sigma}\rangle\rangle\Big), \end{aligned} \tag{A.19}$$

where $\omega_{1,k} = \varepsilon_{k}$ and $\omega_{2,k} = -\varepsilon_{k} + 2\varepsilon_{d} + U$. To obtain $\langle\langle d_{\sigma} n_{d\overline{\sigma}}; d^{\dagger}_{\sigma}\rangle\rangle_{c}$, we apply cluster expansion under spin conservation to Green's functions in equations (A.17)–(A.19). That is,

$$\langle\langle d_{\sigma} n_{d\overline{\sigma}}; d^{\dagger}_{\sigma}\rangle\rangle \sim \langle n_{d\overline{\sigma}}\rangle\langle\langle d_{\sigma}; d^{\dagger}_{\sigma}\rangle\rangle + \langle\langle d_{\sigma} n_{d\overline{\sigma}}; d^{\dagger}_{\sigma}\rangle\rangle_{c}, \tag{A.20}$$

$$\langle\langle c_{\alpha,k,\sigma} n_{d\overline{\sigma}}; d^{\dagger}_{\sigma}\rangle\rangle \sim \langle n_{d\overline{\sigma}}\rangle\langle\langle c_{\alpha,k,\sigma}; d^{\dagger}_{\sigma}\rangle\rangle + \langle\langle c_{\alpha,k,\sigma} n_{d\overline{\sigma}}; d^{\dagger}_{\sigma}\rangle\rangle_{c}, \tag{A.21}$$

$$\begin{aligned} \langle\langle d^{\dagger}_{\overline{\sigma}} c_{\alpha,k,\overline{\sigma}} d_{\sigma}; d^{\dagger}_{\sigma}\rangle\rangle &\sim \langle d^{\dagger}_{\overline{\sigma}} c_{\alpha,k,\overline{\sigma}}\rangle\langle\langle d_{\sigma}; d^{\dagger}_{\sigma}\rangle\rangle \\ &\quad + \langle\langle d^{\dagger}_{\overline{\sigma}} c_{\alpha,k,\overline{\sigma}} d_{\sigma}; d^{\dagger}_{\sigma}\rangle\rangle_{c}, \end{aligned} \tag{A.22}$$

$$\begin{aligned} \langle\langle c^{\dagger}_{\alpha,k,\overline{\sigma}} d_{\overline{\sigma}} d_{\sigma}; d^{\dagger}_{\sigma}\rangle\rangle &\sim \langle c^{\dagger}_{\alpha,k,\overline{\sigma}} d_{\overline{\sigma}}\rangle\langle\langle d_{\sigma}; d^{\dagger}_{\sigma}\rangle\rangle \\ &\quad + \langle\langle c^{\dagger}_{\alpha,k,\overline{\sigma}} d_{\overline{\sigma}} d_{\sigma}; d^{\dagger}_{\sigma}\rangle\rangle_{c}. \end{aligned} \tag{A.23}$$

On the contrary, we neglect all the superconducting correlation functions and pairing correlations obtained from higher-order Green's functions, such as $\langle\langle c^{\dagger}_{\alpha,-k,\overline{\sigma}} n_{d\overline{\sigma}}; d^{\dagger}_{\sigma}\rangle\rangle$, $\langle\langle d^{\dagger}_{\overline{\sigma}} c^{\dagger}_{\alpha,-k,\sigma} d_{\sigma}; d^{\dagger}_{\sigma}\rangle\rangle$, and $\langle\langle c_{\alpha,-k,\sigma} d_{\overline{\sigma}} d_{\sigma}; d^{\dagger}_{\sigma}\rangle\rangle$. Applying these cluster expansions and approximations to (A.16), the final equation composed of the connected part of Green's functions is

$$
\begin{aligned}
&(\omega-\varepsilon_d-U(1-\langle n_{d\bar{\sigma}}\rangle))\langle\langle d_\sigma n_{d\bar{\sigma}};d_\sigma^\dagger\rangle\rangle_c\\
&\quad=U\left[\langle n_{d\bar{\sigma}}\rangle(1-\langle n_{d\bar{\sigma}}\rangle)-\langle d_{\bar{\sigma}}d_\sigma\rangle\langle d_\sigma^\dagger d_{\bar{\sigma}}^\dagger\rangle\right]\langle\langle d_\sigma;d_\sigma^\dagger\rangle\rangle\\
&\qquad+\left[2\varepsilon_d+U(1-\langle n_{d\bar{\sigma}}\rangle+\langle n_{d\sigma}\rangle)\right]\langle d_{\bar{\sigma}}d_\sigma\rangle\langle\langle d_{\bar{\sigma}}^\dagger;d_\sigma^\dagger\rangle\rangle\\
&\qquad+\sum_{\alpha,k}t\Big(\langle\langle c_{\alpha,k,\sigma}n_{d\bar{\sigma}};d_\sigma^\dagger\rangle\rangle_c-\langle\langle c_{\alpha,-k,\bar{\sigma}}^\dagger d_{\bar{\sigma}}d_\sigma;d_\sigma^\dagger\rangle\rangle_c\\
&\qquad+\langle\langle d_{\bar{\sigma}}^\dagger c_{\alpha,-k,\bar{\sigma}}d_\sigma;d_\sigma^\dagger\rangle\rangle_c\Big).
\end{aligned}
\tag{A.24}
$$

To describe $\langle\langle c_{\alpha,k,\sigma}n_{d,\bar{\sigma}};d_\sigma^\dagger\rangle\rangle_c$, $\langle\langle c_{\alpha,-k,\bar{\sigma}}^\dagger d_{\bar{\sigma}}d_\sigma;d_\sigma^\dagger\rangle\rangle_c$, and $\langle\langle d_{\bar{\sigma}}^\dagger c_{\alpha,-k,\bar{\sigma}}d_\sigma;d_\sigma^\dagger\rangle\rangle_c$ in terms of $\langle\langle d_\sigma n_{d\bar{\sigma}};d_\sigma^\dagger\rangle\rangle_c$, we apply the expansions

$$
(\omega-\varepsilon_k)\langle\langle c_{\alpha,k,\sigma}n_{d\bar{\sigma}};d_\sigma^\dagger\rangle\rangle_c\sim t\langle\langle d_\sigma n_{d\bar{\sigma}};d_\sigma^\dagger\rangle\rangle_c,
\tag{A.25}
$$

$$
\begin{aligned}
\left(\omega-\omega_{1,k}\right)\langle\langle d_{\bar{\sigma}}^\dagger c_{\alpha,-k,\bar{\sigma}}d_\sigma;d_\sigma^\dagger\rangle\rangle_c&\sim A_{1,\alpha,k,\sigma}\langle\langle d_\sigma;d_\sigma^\dagger\rangle\rangle\\
&\quad+B_{1,\alpha,k,\sigma}\langle\langle d_\sigma n_{d\bar{\sigma}};d_\sigma^\dagger\rangle\rangle_c,
\end{aligned}
\tag{A.26}
$$

$$
\begin{aligned}
\left(\omega-\omega_{2,k}\right)\langle\langle c_{\alpha,-k,\bar{\sigma}}^\dagger d_{\bar{\sigma}}d_\sigma;d_\sigma^\dagger\rangle\rangle_c&\sim A_{2,\alpha,k,\sigma}\langle\langle d_\sigma;d_\sigma^\dagger\rangle\rangle\\
&\quad-B_{2,\alpha,k,\sigma}\langle\langle d_\sigma n_{d\bar{\sigma}};d_\sigma^\dagger\rangle\rangle_c,
\end{aligned}
\tag{A.27}
$$

where

$$
\begin{aligned}
A_{1,\alpha,k,\sigma}&=\left(\omega_{1,k}-\varepsilon_d-U\langle n_{d\bar{\sigma}}\rangle\right)\langle d_{\bar{\sigma}}^\dagger c_{\alpha,-k,\bar{\sigma}}\rangle+t\langle n_{d\bar{\sigma}}\rangle\\
&\quad-\sum_{k',\alpha'}t\langle c_{\alpha',k',\bar{\sigma}}^\dagger c_{\alpha,-k,\bar{\sigma}}\rangle,\\
A_{2,\alpha,k,\sigma}&=\left(\omega_{2,k}-\varepsilon_d-U\langle n_{d\bar{\sigma}}\rangle\right)\langle c_{\alpha,-k,\bar{\sigma}}^\dagger d_{\bar{\sigma}}\rangle-t\langle n_{d\bar{\sigma}}\rangle\\
&\quad+\sum_{k',\alpha'}t\langle c_{\alpha,-k,\bar{\sigma}}^\dagger c_{\alpha',k',\bar{\sigma}}\rangle,\\
B_{1,\alpha,k,\sigma}&=t-U\langle d_{\bar{\sigma}}^\dagger c_{\alpha,-k,\bar{\sigma}}\rangle,\\
B_{2,\alpha,k,\sigma}&=t+U\langle c_{\alpha,-k,\bar{\sigma}}^\dagger d_{\bar{\sigma}}\rangle.
\end{aligned}
\tag{A.28}
$$

Substituting the approximations of equations (A.25)–(A.27) into equation (A.24), we obtain $\langle\langle d_\sigma n_{d\bar{\sigma}};d_\sigma^\dagger\rangle\rangle_c$. Substituting this result into equation (A.15) with the help of equation (A.14), we finally obtain $\langle\langle d_\sigma;d_\sigma^\dagger\rangle\rangle$ as

$$
\langle\langle d_\sigma;d_\sigma^\dagger\rangle\rangle=\frac{1}{R_\sigma(\omega)-\left(U\left(Q_\sigma(\omega)+T_\sigma(\omega)\right)/P_\sigma(\omega)\right)},
\tag{A.29}
$$

where

$$
\begin{aligned}
P_\sigma(\omega)&=\omega-\varepsilon_d-U\left(1-\langle n_{d\bar{\sigma}}\rangle\right)+3i\Gamma_0\\
&\quad+U\left(A_{1\sigma}(\omega)-A_{2\sigma}(\omega)\right),\\
Q_\sigma(\omega)&=\left(\omega-\varepsilon_d-U\langle n_{d\bar{\sigma}}\rangle\right)\left(A_{1\sigma}(\omega)-A_{2\sigma}(\omega)\right)\\
&\quad+U\left[\langle n_{d\bar{\sigma}}\rangle(1-\langle n_{d\bar{\sigma}}\rangle)-\langle d_{\bar{\sigma}}d_\sigma\rangle\langle d_\sigma^\dagger d_{\bar{\sigma}}^\dagger\rangle\right]\\
&\quad-2i\Gamma_0\langle n_{d\bar{\sigma}}\rangle-\left(B_{1\sigma}(\omega)+B_{2\sigma}(\omega)\right),\\
R_\sigma(\omega)&=\omega-\varepsilon_d-\Sigma_{11}^0(\omega)-U\langle n_{d\bar{\sigma}}\rangle\\
&\quad-\frac{\left(\Sigma_{12}^0(\omega)+U\langle d_{\bar{\sigma}}d_\sigma\rangle\right)\left(\Sigma_{21}^0(\omega)+U\langle d_\sigma^\dagger d_{\bar{\sigma}}^\dagger\rangle\right)}{\omega+\varepsilon_d-\Sigma_{22}^0(\omega)+U\langle n_{d\sigma}\rangle},\\
T_\sigma(\omega)&=\left(2\varepsilon_d+U\left(1+\langle n_{d\sigma}\rangle-\langle n_{d\bar{\sigma}}\rangle\right)\right)\\
&\quad\times\langle d_{\bar{\sigma}}d_\sigma\rangle\frac{\Sigma_{21}^0(\omega)+U\langle d_\sigma^\dagger d_{\bar{\sigma}}^\dagger\rangle}{\omega+\varepsilon_d-\Sigma_{22}^0(\omega)+U\langle n_{d\sigma}\rangle}.
\end{aligned}
\tag{A.30}
$$

In the above, we defined the variables as

$$
\begin{aligned}
A_{i\sigma}&=\sum_{\alpha,k}\frac{t\langle d_{\bar{\sigma}}^\dagger c_{\alpha,-k,\bar{\sigma}}\rangle}{z_+-\omega_{i,k}}\\
&=\frac{i}{2\pi}\sum_{\alpha,k}\frac{1}{z_+-\omega_{i,k}}\int d\omega' f(\omega')t\Big(\langle\langle c_{\alpha,-k,\bar{\sigma}};d_{\bar{\sigma}}^\dagger\rangle\rangle_{\omega'}^r\\
&\quad-\langle\langle c_{\alpha,-k,\bar{\sigma}};d_{\bar{\sigma}}^\dagger\rangle\rangle_{\omega'}^a\Big),
\end{aligned}
\tag{A.31}
$$

where we put $z_+=\omega+i0^+$ and used the spectral theorem $\langle d_{\bar{\sigma}}^\dagger c_{\alpha,-k,\bar{\sigma}}\rangle=(i/2\pi)\int d\omega\, f(\omega)(\langle\langle c_{\alpha,-k,\bar{\sigma}};d_{\bar{\sigma}}^\dagger\rangle\rangle_\omega^r-\langle\langle c_{\alpha,-k,\bar{\sigma}};d_{\bar{\sigma}}^\dagger\rangle\rangle_\omega^a)$ and $\langle c_{\alpha,-k,\bar{\sigma}}^\dagger d_{\bar{\sigma}}\rangle=\langle d_{\bar{\sigma}}^\dagger c_{\alpha,-k,\bar{\sigma}}\rangle$. The expression of $\langle\langle c_{\alpha,k,\bar{\sigma}};d_{\bar{\sigma}}^\dagger\rangle\rangle_\omega^{r(a)}$ is given by

$$
\begin{aligned}
&\langle\langle c_{\alpha,k,\bar{\sigma}};d_{\bar{\sigma}}^\dagger\rangle\rangle_\omega^{r(a)}\\
&\quad=t\frac{(z_\pm+\varepsilon_k)\langle\langle d_{\bar{\sigma}};d_{\bar{\sigma}}^\dagger\rangle\rangle_\omega^{r(a)}-\bar{\sigma}\Delta_\alpha\langle\langle d_\sigma^\dagger;d_{\bar{\sigma}}^\dagger\rangle\rangle_\omega^{r(a)}}{z_\pm^2-\varepsilon_k^2-\Delta^2},
\end{aligned}
\tag{A.32}
$$

where $z_\pm=\omega\pm i0^+$, in which + and − denote the retarded and advanced Green's functions, respectively. Using these expressions, the summation over k in equation (A.31) is given by

$$\sum_k \frac{t\langle\langle c_{\alpha,-k,\overline{\sigma}}; d^{\dagger}_{\overline{\sigma}}\rangle\rangle^{r(a)}_{\omega'}}{z_+ - \omega_{i,k}} = \frac{\Gamma_0}{\pi}\int d\varepsilon \frac{1}{z_+ - \varepsilon_i} \times \frac{(z'_+ + \varepsilon)\langle\langle d_{\overline{\sigma}}; d^{\dagger}_{\overline{\sigma}}\rangle\rangle^{r(a)}_{\omega'} - \overline{\sigma}\Delta_\alpha\langle\langle d^{\dagger}_{\sigma}; d^{\dagger}_{\overline{\sigma}}\rangle\rangle^{r(a)}_{\omega'}}{z'^2_{\pm} - \varepsilon^2 - \Delta^2}, \tag{A.33}$$

where $\varepsilon_1 = \varepsilon$ and $\varepsilon_2 = -\varepsilon + 2\varepsilon_d + U$. Similarly, we defined $B_{i\sigma}$ as

$$B_{i\sigma} = \sum_{\alpha,\alpha',k,k'} \frac{t^2\langle c^{\dagger}_{\alpha',-k',\overline{\sigma}} c_{\alpha,-k,\overline{\sigma}}\rangle}{z_+ - \omega_{i,k}} = \frac{i}{2\pi}\sum_{\alpha,\alpha',k,k'} \frac{1}{z_+ - \omega_{i,k}}\int d\omega' f(\omega') t^2 \times \left(\langle\langle c_{\alpha,-k,\overline{\sigma}}; c^{\dagger}_{\alpha',-k',\overline{\sigma}}\rangle\rangle^{r}_{\omega'} - \langle\langle c_{\alpha,-k,\overline{\sigma}}; c^{\dagger}_{\alpha',-k',\overline{\sigma}}\rangle\rangle^{a}_{\omega'}\right). \tag{A.34}$$

The expression of $\langle\langle c_{\alpha,-k,\overline{\sigma}}; c^{\dagger}_{\alpha',-k',\overline{\sigma}}\rangle\rangle^{r(a)}_{\omega}$ is approximately given as

$$\langle\langle c_{\alpha,-k,\overline{\sigma}}; c^{\dagger}_{\alpha',-k',\overline{\sigma}}\rangle\rangle^{r(a)}_{\omega} = \frac{-\sigma\Delta_\alpha\langle\langle c^{\dagger}_{\alpha,k,\sigma}; c^{\dagger}_{\alpha',-k',\overline{\sigma}}\rangle\rangle^{r(a)}_{\omega} + t\langle\langle d_{\overline{\sigma}}; c^{\dagger}_{\alpha',-k',\overline{\sigma}}\rangle\rangle^{r(a)}_{\omega} + \delta_{\alpha,\alpha'}\delta_{k,k'}}{z_\pm - \varepsilon_{k'}} \sim \frac{t\langle\langle d_{\overline{\sigma}}; c^{\dagger}_{\alpha',-k',\overline{\sigma}}\rangle\rangle^{r(a)}_{\omega} + \delta_{\alpha,\alpha'}\delta_{k,k'}}{z_\pm - \varepsilon_{k'}}, \tag{A.35}$$

with

$$\langle\langle d_\sigma; c^{\dagger}_{\alpha,k,\sigma}\rangle\rangle^{r(a)}_{\omega} = t\frac{(z_\pm + \varepsilon_k)\langle\langle d_\sigma; d^{\dagger}_{\sigma}\rangle\rangle^{r(a)}_{\omega} - \sigma\overline{\Delta}_\alpha\langle\langle d_\sigma; d_{\overline{\sigma}}\rangle\rangle^{r(a)}_{\omega}}{z^2_\pm - \varepsilon^2_k - \Delta^2}. \tag{A.36}$$

In the numerical calculation of the multiple integral in $A_{i,\sigma}$ and $B_{i,\sigma}$, we use the following formulas:

$$I_1 = \int_{-\infty}^{\infty} d\varepsilon \frac{1}{z_+ - \varepsilon}\frac{1}{z'^2_\pm - \varepsilon^2 - \Delta^2} = \begin{cases} \dfrac{\pm\,\mathrm{sgn}(\omega')\pi i}{\sqrt{z'^2_\pm - \Delta^2}}\dfrac{1}{-z_+ \mp \mathrm{sgn}(\omega')\sqrt{z'^2_\pm - \Delta^2}}, & |\omega'| > \Delta, \\ \dfrac{\pi}{\sqrt{\Delta^2 - z'^2_\pm}}\dfrac{1}{-i\sqrt{\Delta^2 - z'^2_\pm} - z_+}, & |\omega'| < \Delta, \end{cases} \tag{A.37}$$

$$I_2 = \int_{-\infty}^{\infty} d\varepsilon \frac{1}{z_+ - \varepsilon}\frac{\varepsilon}{z'^2_\pm - \varepsilon^2 - \Delta^2} = \begin{cases} \dfrac{\pi i}{z_+ \pm \mathrm{sgn}(\omega')\sqrt{z'^2_\pm - \Delta^2}}, & |\omega'| > \Delta, \\ \dfrac{\pi i}{i\sqrt{\Delta^2 - z'^2_\pm} + z_+}, & |\omega'| < \Delta, \end{cases} \tag{A.38}$$

$$I_3 = \int_{-\infty}^{\infty} d\varepsilon \frac{1}{z_+ + \varepsilon - 2\varepsilon_d - U}\frac{1}{z'^2_\pm - \varepsilon^2 - \Delta^2} = \begin{cases} \dfrac{\mp\mathrm{sgn}(\omega')\pi i}{\sqrt{z'^2_\pm - \Delta^2}}\dfrac{1}{z_+ - 2\varepsilon_d - U \pm \mathrm{sgn}(\omega')\sqrt{z'^2_\pm - \Delta^2}}, & |\omega'| > \Delta, \\ \dfrac{-\pi}{\sqrt{\Delta^2 - z'^2_\pm}}\dfrac{1}{i\sqrt{\Delta^2 - z'^2_\pm} + z_+ - 2\varepsilon_d - U}, & |\omega'| < \Delta, \end{cases} \tag{A.39}$$

$$I_4 = \int_{-\infty}^{\infty} d\varepsilon \frac{1}{z_+ + \varepsilon - 2\varepsilon_d - U} \frac{\varepsilon}{z_\pm'^2 - \varepsilon^2 - \Delta^2}$$
$$= \begin{cases} \dfrac{-\pi i}{z_+ - 2\varepsilon_d - U \pm \operatorname{sgn}(\omega')\sqrt{z_\pm'^2 - \Delta^2}}, & |\omega'| > \Delta, \\ \dfrac{-\pi i}{i\sqrt{\Delta^2 - z_\pm'^2} + z_+ - 2\varepsilon_d - U}, & |\omega'| < \Delta. \end{cases} \tag{A.40}$$

In this Lacroix approximation, the higher-order Green's functions in equation (A.16) are expressed in terms of $\langle\langle d_\sigma; d_\sigma^\dagger\rangle\rangle$ and $\langle\langle d_\sigma n_{d\bar\sigma}; d_\sigma^\dagger\rangle\rangle_c$. Eliminating $\langle\langle d_\sigma n_{d\bar\sigma}; d_\sigma^\dagger\rangle\rangle_c$, we calculate $\langle\langle d_\sigma; d_\sigma^\dagger\rangle\rangle$ and $\langle\langle d_{\bar\sigma}^\dagger; d_q^\dagger\rangle\rangle$ self-consistently. In the formulation, $\langle d_\sigma^\dagger c_{\alpha,k,\sigma}\rangle$ and $\langle c_{\alpha,k,\sigma}^\dagger c_{\alpha',k',\sigma}\rangle$ are taken into consideration through $A_{i\sigma}$ and $B_{i\sigma}$, respectively. These terms diverge logarithmically at the Fermi level at zero temperature and play an important role in the Kondo effect [29].

Following similar procedures, we can calculate $\langle\langle d_{\bar\sigma}^\dagger; d_{\bar\sigma}\rangle\rangle$ and $\langle\langle d_\sigma; d_{\bar\sigma}\rangle\rangle$, and the final expressions are

$$\langle\langle d_{\bar\sigma}^\dagger; d_{\bar\sigma}\rangle\rangle = \frac{1}{\widehat{R}_\sigma(\omega) + \left(U\left(\widehat{Q}_\sigma(\omega) + \widehat{T}_\sigma(\omega)\right)/\widehat{P}_\sigma(\omega)\right)}, \tag{A.41}$$

$$\langle\langle d_\sigma; d_{\bar\sigma}\rangle\rangle = \frac{\Sigma_{12}^0(\omega) + U\langle d_{\bar\sigma} d_\sigma\rangle}{\omega - \varepsilon_d - \Sigma_{11}^0(\omega) - U\langle n_{d\bar\sigma}\rangle}\langle\langle d_{\bar\sigma}^\dagger; d_{\bar\sigma}\rangle\rangle, \tag{A.42}$$

where

$$\widehat{P}_\sigma(\omega) = \omega + \varepsilon_d + U\left(1 - \langle n_{d\sigma}\rangle\right) + 3i\Gamma_0 + U\left(\widehat{A}_{1\sigma}(\omega) - \widehat{A}_{2\sigma}(\omega)\right),$$

$$\widehat{Q}_\sigma(\omega) = \left(\omega + \varepsilon_d + U\langle n_{d\sigma}\rangle\right)\left(-\widehat{A}_{1\sigma}(\omega) + \widehat{A}_{2\sigma}(\omega)\right) + U\left[\langle n_{d\sigma}\rangle\left(-1 + \langle n_{d\sigma}\rangle\right) + \langle d_{\bar\sigma} d_\sigma\rangle\langle d_\sigma^\dagger d_{\bar\sigma}^\dagger\rangle\right] - 2i\Gamma_0\langle n_{d\sigma}\rangle - \left(\widehat{B}_{1\sigma}(\omega) + \widehat{B}_{2\sigma}(\omega)\right) - \sigma\Delta\langle d_\sigma^\dagger d_{\bar\sigma}^\dagger\rangle\Gamma_0\left[i\rho_0(\omega) + \left(2\varepsilon_d + U\right)\frac{1}{\pi}\check{I}_3(\omega)\right],$$

$$\widehat{R}_\sigma(\omega) = \omega + \varepsilon_d - \Sigma_{22}^0(\omega) + U\langle n_{d\sigma}\rangle - \frac{\left(\Sigma_{12}^0(\omega) + U\langle d_{\bar\sigma} d_\sigma\rangle\right)\left(\Sigma_{21}^0(\omega) + U\langle d_\sigma^\dagger d_{\bar\sigma}^\dagger\rangle\right)}{\omega - \varepsilon_d - \Sigma_{11}^0(\omega) - U\langle n_{d\bar\sigma}\rangle},$$

$$\widehat{T}_\sigma(\omega) = \left(2\varepsilon_d + U\left(1 + \langle n_{d\bar\sigma}\rangle - \langle n_{d\sigma}\rangle\right)\right) \times \langle d_\sigma^\dagger d_{\bar\sigma}^\dagger\rangle \frac{\Sigma_{12}^0(\omega) + U\langle d_{\bar\sigma} d_\sigma\rangle}{\omega - \varepsilon_d - \Sigma_{11}^0(\omega) - U\langle n_{d\bar\sigma}\rangle}, \tag{A.43}$$

where we defined $\widehat{A}_{i\sigma}(\omega)$, $\widehat{B}_{i\sigma}(\omega)$, and $\check{I}_3(\omega)$ as

$$\widehat{A}_{i\sigma} = \sum_{\alpha,k} \frac{t\langle c_{\alpha,k,\sigma}^\dagger d_\sigma\rangle}{z_+ - \widehat{\omega}_{i,k}} = \frac{i}{2\pi}\sum_{\alpha,k}\frac{1}{z_+ - \widehat{\omega}_{i,k}}\int d\omega' f(\omega') t\Big(\langle\langle d_\sigma; c_{\alpha,k,\sigma}^\dagger\rangle\rangle_{\omega'}^r - \langle\langle d_\sigma; c_{\alpha,k,\sigma}^\dagger\rangle\rangle_{\omega'}^a\Big), \tag{A.44}$$

$$\widehat{B}_{i\sigma} = \sum_{\alpha,\alpha',k,k'} \frac{t^2\langle c_{\alpha,k,\sigma}^\dagger c_{\alpha',k',\sigma}\rangle}{z_+ - \widehat{\omega}_{i,k}} = \frac{i}{2\pi}\sum_{\alpha,\alpha',k,k'}\frac{1}{z_+ - \widehat{\omega}_{i,k}}\int d\omega' f(\omega') t^2 \times \left(\langle\langle c_{\alpha',k',\sigma}; c_{\alpha,k,\sigma}^\dagger\rangle\rangle_{\omega'}^r - \langle\langle c_{\alpha',k',\sigma}; c_{\alpha,k,\sigma}\rangle\rangle_{\omega'}^a\right), \tag{A.45}$$

$$\check{I}_3(\omega) = \int d\varepsilon \frac{1}{z_+ - \widehat{\omega}_2}\frac{1}{z_+^2 - \varepsilon^2 - \Delta^2}, \tag{A.46}$$

where $\widehat{\omega}_{1,k} = -\varepsilon_k$, $\widehat{\omega}_{2,k} = \varepsilon_k - 2\varepsilon_d - U$, $\widehat{\omega}_1 = -\varepsilon$, and $\widehat{\omega}_2 = \varepsilon - 2\varepsilon_d - U$. In the numerical calculation of the multiple integral in $\widehat{A}_{i,\sigma}$ and $\widehat{B}_{i,\sigma}$, we use the following formulas:

$$\widehat{I}_1 = \int_{-\infty}^{\infty} d\varepsilon \frac{1}{z_+ + \varepsilon}\frac{1}{z_\pm'^2 - \varepsilon^2 - \Delta^2} = \begin{cases} \dfrac{\pm\operatorname{sgn}(\omega')\pi i}{\sqrt{z_\pm'^2 - \Delta^2}}\dfrac{1}{-z_+ \pm \operatorname{sgn}(\omega')\sqrt{z_\pm'^2 - \Delta^2}}, & |\omega'| > \Delta, \\ \dfrac{\pi}{\sqrt{\Delta^2 - z_\pm'^2}}\dfrac{1}{i\sqrt{\Delta^2 - z_\pm'^2} - z_+}, & |\omega'| < \Delta, \end{cases} \tag{A.47}$$

$$\widehat{I}_2 = \int_{-\infty}^{\infty} d\varepsilon \frac{1}{z_+ + \varepsilon}\frac{\varepsilon}{z_\pm'^2 - \varepsilon^2 - \Delta^2} = \begin{cases} \dfrac{\pi i}{z_+ \mp \operatorname{sgn}(\omega')\sqrt{z_\pm'^2 - \Delta^2}}, & |\omega'| > \Delta, \\ \dfrac{\pi i}{-i\sqrt{\Delta^2 - z_\pm'^2} + z_+}, & |\omega'| < \Delta, \end{cases} \tag{A.48}$$

$$\widehat{I}_3 = \int_{-\infty}^{\infty} d\varepsilon \frac{1}{z_+ - \varepsilon + 2\varepsilon_d + U} \frac{1}{z_\pm'^2 - \varepsilon^2 - \Delta^2} = \begin{cases} \dfrac{\mp \mathrm{sgn}(\omega')\pi i}{\sqrt{z_\pm'^2 - \Delta^2}} \dfrac{1}{z_+ + 2\varepsilon_d + U \mp \mathrm{sgn}(\omega')\sqrt{z_\pm'^2 - \Delta^2}}, & |\omega'| > \Delta, \\ \dfrac{-\pi}{\sqrt{\Delta^2 - z_\pm'^2}} \dfrac{1}{-i\sqrt{\Delta^2 - z_\pm'^2} + z_+ + 2\varepsilon_d + U}, & |\omega'| < \Delta, \end{cases} \tag{A.49}$$

$$\widehat{I}_4 = \int_{-\infty}^{\infty} d\varepsilon \frac{1}{z_+ - \varepsilon + 2\varepsilon_d + U} \frac{\varepsilon}{z_\pm'^2 - \varepsilon^2 - \Delta^2} = \begin{cases} \dfrac{-\pi i}{z_+ + 2\varepsilon_d + U \mp \mathrm{sgn}(\omega')\sqrt{z_\pm'^2 - \Delta^2}}, & |\omega'| > \Delta, \\ \dfrac{-\pi i}{-i\sqrt{\Delta^2 - z_\pm'^2} + z_+ + 2\varepsilon_d + U}, & |\omega'| < \Delta. \end{cases} \tag{A.50}$$

Data Availability

The data used to support the findings of this study are included within the article.

Conflicts of Interest

The author declares that there are no conflicts of interest.

References

[1] J. C. E. Saldaña, A. Vekris, G. Steffensen et al., "Supercurrent in a double quantum dot," *Physical Review Letters*, vol. 121, no. 25, Article ID 257701, 2018.

[2] D. J. Luitz, F. F. Assaad, T. Novotný, C. Karrasch, and V. Meden, "Understanding the Josephson current through a Kondo-correlated quantum dot," *Physical Review Letters*, vol. 108, no. 22, Article ID 227001, 2012.

[3] J. A. van Dam, Y. V. Nazarov, E. P. A. M. Bakkers, S. De Franceschi, and L. P. Kouwenhoven, "Supercurrent reversal in quantum dots," *Nature*, vol. 442, no. 7103, pp. 667–670, 2006.

[4] H. I. Jorgensen, T. Novotný, K. Grove-Rasmussen, K. Flensberg, and P. E. Lindelof, "Critical current 0–π transition in designed Josephson quantum dot junctions," *Nano Letters*, vol. 7, no. 8, pp. 2441–2445, 2007.

[5] A. Barone and G. Paternò, *Physics and Applications of the Josephson Effect*, John Wiley & Sons Inc., New York, NY, USA, 1982.

[6] B.-K. Kim, Y.-H. Ahn, J.-J. Kim et al., "Transport measurement of Andreev bound states in a Kondo-correlated quantum dot," *Physical Review Letters*, vol. 110, no. 7, Article ID 076803, 2013.

[7] A. Eichler, M. Weiss, S. Oberholzer et al., "Even-odd effect in Andreev transport through a carbon nanotube quantum dot," *Physical Review Letters*, vol. 99, no. 12, Article ID 126602, 2007.

[8] R. Maurand, T. Meng, E. Bonet, S. Florens, L. Marty, and W. Wernsdorfer, "First-order 0–π quantum phase transition in the Kondo regime of a superconducting carbon-nanotube quantum dot," *Physical Review X*, vol. 2, no. 1, Article ID 011009, 2012.

[9] K. Osawa, S. Kurihara, and N. Yokoshi, "Fano effect in a Josephson junction with a quantum dot," *Physical Review B: Condensed Matter and Materials Physics*, vol. 78, no. 22, Article ID 224508, 2008.

[10] J.-P. Cleuziou, W. Wernsdorfer, V. Bouchiat, T. Ondarçuhu, and M. Monthioux, "Carbon nanotube superconducting quantum interference device," *Nature Nanotechnology*, vol. 1, no. 1, pp. 53–59, 2006.

[11] G. Sellier, T. Kopp, J. Kroha, and Y. S. Barash, "π junction behavior and Andreev bound states in Kondo quantum dots with superconducting leads," *Physical Review B: Condensed Matter and Materials Physics*, vol. 72, no. 17, Article ID 174502, 2005.

[12] F. Dolcini and F. Giazotto, "Switching the sign of Josephson current through Aharonov-Bohm interferometry," *Physical Review B: Condensed Matter and Materials Physics*, vol. 75, no. 14, Article ID 140511(R), 2007.

[13] M.-S. Choi, M. Lee, K. Kang, and W. Belzig, "Kondo effect and Josephson current through a quantum dot between two superconductors," *Physical Review B: Condensed Matter and Materials Physics*, vol. 70, no. 2, Article ID 020502(R), 2004.

[14] T. Domański, M. Žonda, V. Pokorný, G. Górski, V. Janiš, and T. Novotný, "Josephson-phase-controlled interplay between correlation effects and electron pairing in a three-terminal nanostructure," *Physical Review B: Condensed Matter and Materials Physics*, vol. 95, no. 4, Article ID 045104, 2017.

[15] C. Ishii, "Josephson currents through junctions with normal metal barriers," *Progress of Theoretical Physics*, vol. 44, no. 6, pp. 1525–1547, 1970.

[16] S.-G. Cheng, Y. X. Xing, X. C. Xie, and Q. F. Sun, "Supercurrent and its Fano effect in a Josephson Aharonov-Bohm ring," *The European Physical Journal B: Condensed Matter and Complex Systems*, vol. 67, no. 4, pp. 551–557, 2009.

[17] J. Martinek, M. Sindel, L. Borda et al., "Kondo effect in the presence of itinerant-electron ferromagnetism studied with the numerical renormalization group method," *Physical Review Letters*, vol. 91, no. 24, Article ID 247202, 2003.

[18] M.-S. Choi, D. Sánchez, and R. López, "Kondo effect in a quantum dot coupled to ferromagnetic leads: a numerical renormalization group analysis," *Physical Review Letters*, vol. 92, no. 5, Article ID 056601, 2004.

[19] J. Bauer, A. Oguri, and A. C. Hewson, "Spectral properties of locally correlated electrons in a Bardeen-Cooper-Schrieffer superconductor," *Journal of Physics: Condensed Matter*, vol. 19, no. 48, Article ID 486211, 2007.

[20] K. Haule, S. Kirchner, J. Kroha, and P. Wölfle, "Anderson impurity model at finite Coulomb interaction U: generalized noncrossing approximation," *Physical Review B: Condensed Matter and Materials Physics*, vol. 64, no. 15, Article ID 155111, 2001.

[21] P. Werner, A. Comanac, L. de' Medici, M. Troyer, and A. J. Millis, "Continuous-time solver for quantum impurity models," *Physical Review Letters*, vol. 97, no. 7, Article ID 076405, 2006.

[22] A. N. Rubtsov, V. V. Savkin, and A. I. Lichtenstein, "Continuous-time quantum Monte Carlo method for fermions," *Physical Review B: Condensed Matter and Materials Physics*, vol. 72, no. 3, Article ID 035122, 2005.

[23] F. Siano and R. Egger, "Josephson current through a nanoscale magnetic quantum dot," *Physical Review Letters*, vol. 93, no. 4, Article ID 047002, 2004.

[24] E. Vecino, A. Martín-Rodero, and A. L. Yeyati, "Josephson current through a correlated quantum level: Andreev states and π junction behavior," *Physical Review B: Condensed Matter and Materials Physics*, vol. 68, no. 3, Article ID 035105, 2003.

[25] J. C. Cuevas, A. L. Yeyati, and A. Martín-Rodero, "Kondo effect in normal-superconductor quantum dots," *Physical Review B: Condensed Matter and Materials Physics*, vol. 63, no. 9, Article ID 094515, 2001.

[26] C. Benjamin, T. Jonckheere, A. Zazunov, and T. Martin, "Controllable π junction in a Josephson quantum-dot device with molecular spin," *The European Physical Journal B: Condensed Matter and Complex Systems*, vol. 57, no. 3, pp. 279–289, 2007.

[27] S. Kawaguchi, "Spin-flip effects on current in a quantum dot with a Josephson junction system," *Journal of the Physical Society of Japan*, vol. 81, no. 3, Article ID 034707, 2012.

[28] H.-G. Luo, Z.-J. Ying, and S.-J. Wang, "Equation of motion approach to the solution of the Anderson model," *Physical Review B: Condensed Matter and Materials Physics*, vol. 59, no. 15, pp. 9710–9713, 1999.

[29] C. Lacroix, "Density of states for the Anderson model," *Journal of Physics F: Metal Physics*, vol. 11, no. 11, pp. 2389–2397, 1981.

[30] Y. Qi, J.-X. Zhu, S. Zhang, and C. S. Ting, "Kondo resonance in the presence of spin-polarized currents," *Physical Review B: Condensed Matter and Materials Physics*, vol. 78, no. 4, Article ID 045305, 2008.

[31] J. S. Lim, R. López, L. Limot, and P. Simon, "Nonequilibrium spin-current detection with a single Kondo impurity," *Physical Review B: Condensed Matter and Materials Physics*, vol. 88, no. 16, Article ID 165403, 2013.

[32] L. Li, Z. Cao, H.-G. Luo, F.-C. Zhang, and W.-Q. Chen, "Fano resonance in a normal metal/ferromagnet-quantum dot-superconductor device," *Physical Review B: Condensed Matter and Materials Physics*, vol. 92, no. 19, Article ID 195155, 2015.

[33] L. Li, M.-X. Gao, Z.-H. Wang, H.-G. Luo, and W.-Q. Chen, "Rashba-induced Kondo screening of a magnetic impurity in a two-dimensional superconductor," *Physical Review B: Condensed Matter and Materials Physics*, vol. 97, no. 6, Article ID 064519, 2018.

[34] M. Ţolea, I. V. Dinu, and A. Aldea, "Kondo peaks and dips in the differential conductance of a multi-lead quantum dot: dependence on bias conditions," *Physical Review B: Condensed Matter and Materials Physics*, vol. 79, no. 3, Article ID 033306, 2009.

[35] L. Li, B.-B. Zheng, W.-Q. Chen, H. Chen, H.-G. Luo, and F.-C. Zhang, "0–π transition characteristic of the Josephson current in a carbon nanotube quantum dot," *Physical Review B: Condensed Matter and Materials Physics*, vol. 89, no. 24, Article ID 245135, 2014.

[36] R. Bulla, A. C. Hewson, and T. Pruschke, "Numerical renormalization group calculations for the self-energy of the impurity Anderson model," *Journal of Physics: Condensed Matter*, vol. 10, no. 37, pp. 8365–8380, 1998.

[37] A. P. Jauho, N. S. Wingreen, and Y. Meir, "Time-dependent transport in interacting and noninteracting resonant-tunneling systems," *Physical Review B: Condensed Matter and Materials Physics*, vol. 50, no. 8, pp. 5528–5544, 1994.

[38] Y. Meir and N. S. Wingreen, "Landauer formula for the current through an interacting electron region," *Physical Review Letters*, vol. 68, no. 16, pp. 2512–2515, 1992.

[39] Q.-F. Sun, B.-G. Wang, J. Wang, and T.-H. Lin, "Electron transport through a mesoscopic hybrid multiterminal resonant-tunneling system," *Physical Review B: Condensed Matter and Materials Physics*, vol. 61, no. 7, pp. 4754–4761, 2000.

[40] H. Haug and A.-P. Jauho, *Quantum Kinetics in Transport and Optics of Semiconductors*, Springer-Verlag, Berlin, Germany, 2nd edition, 2008.

[41] R. van Roermund, *Theoretical study of non-equilibrium transport in Kondo quantum dots*, Ph.D. thesis, Université de Grenoble, Grenoble, France, 2010.

[42] L. N. Bulaevskii, V. V. Kuzii, and A. A. Sobyanin, "Superconducting system with weak coupling to the current in the ground state," *JETP Letters*, vol. 25, no. 7, pp. 290–294, 1977.

[43] F. D. M. Haldane, "Scaling theory of the asymmetric Anderson model," *Physical Review Letters*, vol. 40, no. 6, pp. 416–419, 1978.

[44] J. S. Lim, M.-S. Choi, M. Y. Choi, R. López, and R. Aguado, "Kondo effects in carbon nanotubes: from SU(4) to SU(2) symmetry," *Physical Review B: Condensed Matter and Materials Physics*, vol. 74, no. 20, Article ID 205119, 2006.

[45] T.-F. Fang, W. Zuo, and H.-G. Luo, "Kondo effect in carbon nanotube quantum dots with spin-orbit coupling," *Physical Review Letters*, vol. 101, no. 24, Article ID 246805, 2008.

[46] H. Pan and T.-H. Lin, "Spin-flip effects on the supercurrent through mesoscopic superconducting junctions," *Journal of Physics: Condensed Matter*, vol. 17, no. 34, pp. 5207–5214, 2005.

[47] Y. Zhu, Q. F. Sun, and T. H. Lin, "Andreev bound states and the π-junction transition in a superconductor/quantum-dot/superconductor system," *Journal of Physics: Condensed Matter*, vol. 13, no. 39, pp. 8783–8798, 2001.

[48] C. Karrasch, A. Oguri, and V. Meden, "Josephson current through a single Anderson impurity coupled to BCS leads," *Physical Review B: Condensed Matter and Materials Physics*, vol. 77, no. 2, Article ID 024517, 2008.

[49] L. Li, Z. Cao, T.-F. Fang, H.-G. Luo, and W.-Q. Chen, "Kondo screening of Andreev bound states in a normal metal-quantum dot-superconductor system," *Physical Review B: Condensed Matter and Materials Physics*, vol. 94, no. 16, Article ID 165144, 2016.

[50] J. Barański and T. Domański, "Fano-type interference in quantum dots coupled between metallic and superconducting leads," *Physical Review B: Condensed Matter and Materials Physics*, vol. 84, no. 19, Article ID 195424, 2011.

[51] J. Barański and T. Domański, "In-gap states of a quantum dot coupled between a normal and a superconducting lead," *Journal of Physics: Condensed Matter*, vol. 25, no. 43, Article ID 435305, 2013.